arXiv:1201.1782v2 [q-fin.PR] 11 Jan 2012

Smiles all around: FX joint calibration in a multi-Heston model

Alvise De Col* Alessandro Gnoatto† Martino Grasselli‡

January 12, 2012

Abstract

Multi-currency FX derivatives offer a challenging playground to the mathematical modelling of correlations. Quotes of liquidly traded vanilla options on cross FX rates, e.g. EUR/JPY, can be used to extract a great deal of information about the complex implied correlation structure between the corresponding main FX rates, e.g. USD/JPY and EUR/USD. Including all this information in a financial model means being able to fit simultaneously all volatility smiles, a very demanding task. In this paper we propose a first solution to this problem in the class of stochastic volatility models. We introduce a novel multi-factor stochastic volatility Heston-based model, which is able to reproduce consistently typical multi-dimensional FX vanilla markets, while retaining the (semi)-analytical tractability typical of affine models and relying on a reasonable number of parameters. A successful joint calibration to real market data is presented together with various in- and out-of-sample calibration exercises to highlight the robustness of the parameters estimation. The proposed model is symmetric with respect to the choice of the risk-free currency, opening up to new approaches for coherent pricing and risk management of derivatives depending on multiple currencies.

1 Introduction

Derivatives with multiple underlying components have attracted in recent times an increasing amount of attention, partly in form of public scrutiny and criticisms. Their popularity extends to the different asset classes traded in the financial markets, ranging from basket options written on equity stocks and foreign exchange rates, to CDO structures on various fixed income instruments and complex hybrid structures combining the different underlying types (see

---

[*] UBS-AG, UBS, Europastrasse 1, 8152 Opfikon, (Switzerland)

[†] Dipartimento di Matematica, Padova (Italy) and Mathematisches Institut, LMU München (Germany)

[‡] Dipartimento di Matematica, Padova (Italy) and Département Mathématiques et Ingénierie Financière, ESILV, Paris La Défense (France). Acknowledgements: we are grateful to Jan Baldeaux, Damiano Brigo, Imran Hafeez, Eckhard Platen, Wolfgang Runggaldier for useful comments.

e.g. [Wystup, 2006], [Clark, 2011], [Esquível et al., 2010]). From a client perspective the appeal of such structures is clear and understandable: diversification reduces the exposure to individual components while the whole structure is cheaper to buy than multiple single-underlying options [Qu, 2010]. The correlations between the returns of the different components are the key inputs in the determination of this rebate. Most often, however, these correlations are not observable in the market; a fact that leads to material uncertainties and complications in the valuation and risk management of, even rather standard, multi-component derivatives.

There is nevertheless a notable and mostly overlooked example, in which much can be said from the market about the correlation structure. This is often the case of derivatives with multiple underlying FX rates (see [Esquível et al., 2010]). Rather paradoxically, here we face the opposite problem: instead of having little evidence on where correlations trade, the market gives many indications on their structure, potentially more than any standard model, like a copula model, can handle. This information can be extracted from the liquid vanilla markets and the fact that, differently from other asset classes, appropriate multiplication/division of FX rates are still FX rates, and hence directly observable through standard FX spot transactions. To capture the market correlation structure we need a model that is able to price consistently vanilla options across different FX pairs (see e.g. [Castagna, 2010], [Beneder and Elkenbracht-Huizing, 2003]). At the same time, given the high dimensionality of the problem, for any possible practical application we seek to retain some kind of analytical tractability. In this paper, we present a first proposal of such a model.

The focus of our analysis is on the simultaneous calibration of several FX vanilla surfaces. This is indeed an important model prerequisite for pricing structures with multiple underlying FX rates. For the sake of simplicity, let us consider as an example the FX market composed by three currencies: say Euro (EUR), US dollar (USD), and Japanese Yen (JPY). All three currency pairs EUR/USD, USD/JPY, and EUR/JPY are liquidly traded, both as FX spot transactions and vanilla FX options. Let $S^{\mathrm{d,f}}(t)$ be the spot exchange rate at time t as the amount of domestic (d) currency for one unit of foreign currency (f). As a consequence of the standard triangular relationship between the FX rates, e.g. $S^{\mathrm{JPY,EUR}}(t) = S^{\mathrm{JPY,USD}}(t)S^{\mathrm{USD,EUR}}(t)$, the price of a multi-dimensional option on any of the two of the three pairs is also *implicitly* sensitive to the volatility of the excluded pair. This fact is easily understood in the case of no-skew. To fix ideas let us consider a basket option on EUR/USD and USD/JPY. The correlation between the two main FX rates $\rho_{\mathrm{EUR/USD-USD/JPY}}$ can be derived from the volatility of the cross via the triangular relation (see e.g. [Clark, 2011] p. 228)

$$\rho_{\mathrm{EUR/USD-USD/JPY}} = \frac{\sigma^2_{\mathrm{EUR/JPY}} - \sigma^2_{\mathrm{EUR/USD}} - \sigma^2_{\mathrm{USD/JPY}}}{2\sigma_{\mathrm{EUR/USD}}\sigma_{\mathrm{USD/JPY}}}. \tag{1}$$

By varying the cross volatility $\sigma_{\mathrm{EUR/JPY}}$ and keeping the main volatilities fixed, one can span over any value of the correlation between -1 and 1, yielding significantly different values for the basket structure.

Similarly, if the volatility skew is included, the basket structure becomes sensitive to *all* three volatility smiles. A good pricing model must be able to reproduce all three vanilla markets; theoretically, a very challenging prerequisite.

The easiest way to proceed is to calibrate the volatility smiles of the two main currency pairs using typical unidimensional models and try to obtain the third from the correlation between them. If, however, we stick to a simple mathematical modelling of the correlation, say either constant or time-dependent, we face two problems. Firstly, a simultaneous calibration to all volatility smiles in the triangle is in general difficult to obtain, as a constant correlation does not provide enough flexibility to match the smile of the FX cross. Secondly, the model is not functionally symmetric with respect to which FX pairs we choose to be the main ones and which one the cross. In other terms, the stochastic process of the cross FX rate is functionally different from the processes of the main FX rates it is derived from.

This latter point, although theoretical at first sight, is of key practical importance. In principle we have the freedom of choosing any of the currencies as our numéraire when pricing a multi-currency structure (although some choices are more natural than others, e.g. the payout currency which is specified in the contract). A model that is able to treat symmetrically all currencies must be therefore preferred. Two approaches in this direction have been proposed in [Doust, 2007] and [Carr and Verma, 2005]. The main purpose of this paper is to specify a model with this property in the class of multi-dimensional stochastic volatility models. To achieve our goal, we need a paradigm change in the model specification. We have to forgo the standard approach of leaving the task of matching the volatility skew of the cross FX rate to the correlation between the main exchange rates. Instead of putting the currency pairs at the basis of our model, we start from the observation that any exchange rate may be seen as a ratio between two quantities, the value of the currencies with respect to some universal numéraire, and include this feature in the specification of the model: this reflects the point of view of the Benchmark approach in [Heath and Platen, 2006b] and [Heath and Platen, 2006a]. In this way, our model does not change qualitatively depending on which perspective is used. The benefits of this property are manifold: *i)* the calibration is universal, i.e., it is independent on the exotic product being priced (due to the symmetry of the numéraire currency), *ii)* the price of the exotic will not vary depending on which perspective is chosen; moreover, *iii)* the model produces symmetric and consistent risk sensitivities with possibly positive impacts on the way multi-dimensional option books can be risk managed.

The model we present in this paper is a multi-factor stochastic volatility model of Heston type [Heston, 1993], which extends the standard approach in [Garman and Kohlhagen, 1983]. The Heston dynamics leads to an affine model which is known to retain analytical tractability. We will provide a complete discussion concerning the set of risk neutral measures and the rules to change between them. Rather remarkably, as a consequence of the specific Heston-type dynamics, the model remains functionally invariant, after parameter rescaling, when the risk-neutral measure is changed. This is key feature that allows obtaining an universal calibration with reasonable computational effort. We will then test the model on real market data and show how a joint calibration of the volatility smiles of EUR/USD/JPY triangle is possible. In- and out-of-sample calibration tests will be reported to comment on the robustness of the parameter estimation.

The paper is organized as follows: we present the model in Sect. 2, initially using the perspective given by some kind of universal numéraire. We continue with the basic properties of the model, such as the positivity of the instantaneous covariance matrix and the presence of stochastic skewness, before presenting the invariance of the model and transformation rule of its parameters when the risk neutral measure is changed in Sect. 3. The explicit formulae for the characteristic function and option prices are given in Sect. 4 before turning to the small vol-of-vol expansions of the option prices and implied volatilities in Sect. 5. Finally, the joint calibration to EUR/USD/JPY market volatility smiles is presented in Sect. 6, together with a discussion of the procedure and the results, including the Feller condition and moment explosion.

2 Multifactor Heston-based exchange model

We consider a foreign exchange market in which N currencies are traded between each other via standard FX spot and FX vanilla option transactions. We start by considering the value of each of these currencies in units of a universal numéraire. We will see that the discussion is independent on the exact specification of this numéraire. To fix the ideas, one can think of it as a precious metal, e.g. gold, or the market portfolio like in the benchmark approach of [Heath and Platen, 2006b] and [Heath and Platen, 2006a].

Let us work in the risk neutral measure defined by the universal numéraire and call $S^{0,i}(t)$ the value at time t of one unit of the currency i in terms of our universal numéraire (note that $S^{0,i}(t)$ can itself be thought as an exchange rate, between the universal numéraire and the currency i). We model each of the $S^{0,i}(t)$ via a multi-variate Heston stochastic volatility model [Heston, 1993] with d independent Cox-Ingersoll-Ross (CIR) components [Cox et al., 1985], $\mathbf{V}(t) \in \mathbb{R}^d$, and an equivalent number of driving noises, $\mathbf{Z}(t) \in \mathbb{R}^d$. The dimension d can be chosen according to the specific problem and may reflect a PCA-type analysis. We further assume that these stochastic volatility components are *common* between the different $S^{0,i}(t)$. Formally, we write

$$\frac{dS^{0,i}(t)}{S^{0,i}(t)} = (r^0 - r^i)dt - (\mathbf{a}^i)^\top \mathrm{Diag}(\sqrt{\mathbf{V}(t)})d\mathbf{Z}(t), \qquad i = 1, \dots, N; \tag{2}$$

$$dV_k(t) = \kappa_k(\theta_k - V_k(t))dt + \xi_k \sqrt{V_k(t)}dW_k(t), \qquad k = 1, \dots, d; \tag{3}$$

where $\kappa_k, \theta_k, \xi_k \in \mathbb{R}$ are standard parameters in a CIR dynamics. $\mathrm{Diag}(\sqrt{\mathbf{V}(t)})$ denotes the diagonal matrix with the square root of the elements of the vector $\mathbf{V}(t)$ in the principal diagonal, this term is multiplied with the linear vector $\mathbf{a}^i \in \mathbb{R}^d$ $(i = 1, \dots, N)$; as a result, the dynamics of the exchange rate is driven by a linear projection of the variance factor $\mathbf{V}(t)$ along a direction parametrized by $\mathbf{a}^i$, namely the total instantaneous variance is $(\mathbf{a}^i)^\top \mathrm{Diag}(\mathbf{V}(t))\mathbf{a}^i dt$. In each monetary area i, the money-market account accrues interest based on the deterministic risk free rate r^i,

$$dB^i(t) = r^i B^i(t)dt, \qquad i = 1, \dots, N; \tag{4}$$

in our gold analogy r^0 is the precious metal lease rate. Finally, we assume an orthogonal correlation structure between the stochastic drivers

$$\langle dZ_k(t)dW_h(t)\rangle = \rho_k \delta_{kh} dt, \quad k,h = 1,\dots,d, \tag{5}$$

together with $\langle dZ_k(t)dZ_h(t)\rangle = \delta_{kh}dt$ and $\langle dW_k(t)dW_h(t)\rangle = \delta_{kh}dt$.
This concludes the description of our model.

The idea behind this approach is that each exchange rate is driven by several independent drivers $dZ_k(t)$ $(k = 1,..,d)$, each with an independent stochastic variance factor $V_k(t)$, to which $dZ_k(t)$ is partially correlated via ρ_k. The vectors $\mathbf{a}^i$ $(i = 1,\dots,N)$ describe by how much each of the different volatilities contribute to the dynamics of $S^{0,i}(t)$. This correlation structure is responsible for the appearance of non-standard effects in the model, like a stochastic skewness, see subsection 2.3.

All in all, we have introduced a total number of parameters equal to $N_{\mathrm{P}} = Nd + 5d$ (Nd from the vectors $\mathbf{a}^i$ and 5 for each CIR process, $\kappa_k, \theta_k, \xi_k, \rho_k$ and the initial value $V_k(0)$) to describe the volatility skew of $(N^2 - N)/2$ currency pairs. As rule of thumb, assuming that each currency pair can be approximately modeled by a standard one-dimensional Heston model, which is described by 5 parameters, around $5(N^2 - N)/2$ parameters are needed to fit all volatility surfaces; the value of d should be chosen to produce approximately this number of parameters, if not less, to avoid instabilities due to overfitting.

Let us now turn our attention to the exchange rate $S^{i,j}(t)$ between two different currencies, say i and j. We set by definition $S^{i,j}(t) := S^{0,j}(t)/S^{0,i}(t)$. By straightforward calculation, we obtain for $i,j = 1,..,N$:

$$\frac{dS^{i,j}(t)}{S^{i,j}(t)} = (r^i - r^j)dt + (\mathbf{a}^i - \mathbf{a}^j)^\top \mathrm{Diag}(\mathbf{V}(t))\mathbf{a}^i dt + (\mathbf{a}^i - \mathbf{a}^j)^\top \mathrm{Diag}(\sqrt{\mathbf{V}(t)})d\mathbf{Z}(t). \tag{6}$$

Note that at this stage we are still working under the risk neutral measure defined by the universal numéraire. The additional drift term in (6) can be understood as a quanto adjustment between the currency 0 and i.

Proposition 1. *The dynamics of the exchange rate (2) satisfies the triangular relation, namely for all* $t \geq 0$ *and* $i,j,l = 1,..,N$*:*

$$dS^{i,j}(t) = d\left(S^{i,l}(t)S^{l,j}(t)\right). \tag{7}$$

Proof. Straightforward application of Ito's rule. □

This symmetry property is fundamental in order to have a model that yields universal calibration and consistent pricing of exotic options. In the following subsections, we will analyze some additional properties of the model and familiarize with the meaning of the different parameters.

2.1 Vectors $\mathbf{a}^i$ cannot be the canonical basis

A rather natural choice would be to set $\mathbf{a}^i$ equal to the canonical basis $\mathbf{e}^i$ (i.e. the i-th element of the canonical basis of $\mathbb{R}^N$, $e^i_l = \delta_{li},\ i,l = 1,..,N$), then (6), for $i \neq j$, reads:

$$\frac{dS^{i,j}(t)}{S^{i,j}(t)} = (r^i - r^j)dt + V^i(t)dt + \sqrt{V_i(t)}dZ^i(t) - \sqrt{V_j(t)}dZ^j(t), \tag{8}$$

which in the 3-currency case leads to the 3-factor Heston model. The problem with this choice is that the covariances (and thus the correlations) between different pairs are forced to be positive,

$$\left\langle \frac{dS^{i,j}(t)}{S^{i,j}(t)}, \frac{dS^{i,l}(t)}{S^{i,l}(t)} \right\rangle = V^i(t)dt \geq 0. \tag{9}$$

As we need the flexibility to define negative correlation between FX rates, the vectors $\mathbf{a}^i$ cannot be taken equal to the canonical basis. These additional parameters are needed to describe a multi-dimensional FX market.

2.2 Stochastic covariance matrix

By construction, the model (2) has a stochastic instantaneous $(N-1) \times (N-1)$ covariance matrix. We prove here that the specification of the model always leads to a positive definite covariance matrix, a fundamental prerequisite for any well-posed multi-dimensional model. For example, we consider the case of three currencies and the associated 2×2 candidate covariance matrix where we fix the point of view of currency i:

$$\mathrm{Cov}^i(t) = \begin{pmatrix} \left\langle \frac{dS^{i,j}(t)}{S^{i,j}(t)} \right\rangle & \left\langle \frac{dS^{i,j}(t)}{S^{i,j}(t)}, \frac{dS^{i,l}(t)}{S^{i,l}(t)} \right\rangle \\ \left\langle \frac{dS^{i,j}(t)}{S^{i,j}(t)}, \frac{dS^{i,l}(t)}{S^{i,l}(t)} \right\rangle & \left\langle \frac{dS^{i,l}(t)}{S^{i,l}(t)} \right\rangle \end{pmatrix}, \tag{10}$$

where

$$\left\langle \frac{dS^{i,j}(t)}{S^{i,j}(t)}, \frac{dS^{i,l}(t)}{S^{i,l}(t)} \right\rangle = \left(\mathbf{a}^i - \mathbf{a}^j\right)^\top \mathrm{Diag}(\mathbf{V}(t)) \left(\mathbf{a}^i - \mathbf{a}^l\right) dt. \tag{11}$$

Variances, i.e., the diagonal terms in the covariance matrix, are clearly positive due to the positiveness of $V_k(t), k = 1, .., d$. To prove that the whole covariance matrix is positive definite, it is sufficient to introduce the $(N-1) \times d$ matrix B defined as follows:

$$B_{j,k} := a_k^j - a_k^1; \quad k = 1, .., d; \quad j = 2, \dots, N, \tag{12}$$

where without loss of generality we can take the point of view of currency $i = 1$. With this notation the $(N-1) \times (N-1)$ variance/covariance matrix $\mathrm{Cov}^1(t) = \mathrm{Cov}(t)$ is given by

$$\mathrm{Cov}(t) = B\,\mathrm{Diag}(\mathbf{V}(t))B^\top, \tag{13}$$

which is positive semidefinite since for all $\mathbf{x} \in \mathbb{R}^d$:

$$\mathbf{x}^\top \mathrm{Cov}(t)\mathbf{x} = (B^\top \mathbf{x})^\top \mathrm{Diag}(\mathbf{V}(t))B^\top \mathbf{x} \geq 0,$$

where the last inequality follows from the positive definiteness of the matrix $\mathrm{Diag}(\mathbf{V}(t))$.

In conclusion the variance-covariance matrix is well defined, and, as an important side effect, we have the usual bound for the correlations, i.e. all correlations are bounded by one in absolute value.

2.3 Stochastic Skew

To shed some additional light on the meaning of the vectors $\mathbf{a}^i$ we calculate the skewness ς for a given exchange rate $S^{i,j}$, defined as the correlation between the log returns and the stochastic variance:

$$\varsigma^{i,j}(t) = \frac{\langle \mathrm{Noise}(\log S^{i,j}), \mathrm{Noise}(\mathrm{Vol}(\log S^{i,j}))\rangle_t}{\sqrt{\langle (\mathrm{Noise}(\log S^{i,j}))\rangle_t}\sqrt{\langle (\mathrm{Noise}(\mathrm{Vol}(\log S^{i,j})))\rangle_t}}. \tag{14}$$

Differently from standard single factor models, multifactor Heston models produce a stochastic skewness. In fact, by straightforward calculation we obtain:

$$\begin{aligned} \left\langle d\log S^{i,j}, dV_k \right\rangle_t &= \left\langle \sum_{l=1}^{d} \left(\mathbf{a}^i_l - \mathbf{a}^j_l\right) \sqrt{V_l} dZ_l, \xi_k \sqrt{V_k} \rho_k dZ_k \right\rangle_t \\ &= \left(a^i_k - a^j_k\right) \xi_k V_k(t) \rho_k dt \qquad i,j = 1,..,N;\ k = 1,...,d. \end{aligned} \tag{15}$$

Combining this term with

$$\left\langle d\log S^{i,j}, d\log S^{i,j} \right\rangle_t = \left(\mathbf{a}^i - \mathbf{a}^j\right)^\top \mathrm{Diag}(\mathbf{V}(t)) \left(\mathbf{a}^i - \mathbf{a}^j\right) dt$$

and $\langle dV_k, dV_k \rangle_t = \xi_k^2 V_k(t) dt$, we obtain

$$\varsigma^{i,j}(t) = \frac{\sum_{k=1}^{d} \left(a^i_k - a^j_k\right) \xi_k V_k(t) \rho_k}{\sqrt{\sum_{k=1}^{d} \xi_k^2 V_k(t)} \sqrt{\left(\mathbf{a}^i - \mathbf{a}^j\right)^\top \mathrm{Diag}(\mathbf{V}(t)) \left(\mathbf{a}^i - \mathbf{a}^j\right)}}. \tag{16}$$

This quantity is stochastic due to the presence of the variance factors $V_k(t)$, $k = 1,..,d$ [Christoffersen et al., 2009]. The vectors $\mathbf{a}^i$ are directly related to the amount of skewness for each of the different exchange rates.

3 Numéraire invariance

Up to now we have worked under the risk neutral measure defined by our (rather unspecified) universal numéraire. In practical pricing applications, it is more convenient to change the numéraire to any of the currencies included in our FX multi-dimensional system. Without loss of generality, let us consider the risk neutral measure defined by the i-th money market account $B^i(t)$ and derive the dynamical equations for the standard FX rate $S^{i,j}(t)$, its inverse $S^{j,i}(t)$, and a generic cross $S^{j,l}(t)$ for $i, j, l = 1,..,N$.

Under the assumptions of the fundamental theorem of asset pricing (cfr. e.g. [Björk, 2009], chapters 13 and 14), investing domestic money into any foreign currency money-market account cannot produce a risk free return different from r^i. In other terms, the ratio $S^{i,j}(t)B^j(t)/B^i(t)$ must be a local martingale under the i-th risk free measure $\mathbb{Q}^i$, provided that such risk neutral measure exists. Hence,

$$\begin{aligned} d\left(\frac{S^{i,j}(t)B^j(t)}{B^i(t)}\right) &= \frac{S^{i,j}(t)B^j(t)}{B^i(t)} \left((\mathbf{a}^i - \mathbf{a}^j)^\top \mathrm{Diag}(\mathbf{V}(t)) \mathbf{a}^i dt + (\mathbf{a}^i - \mathbf{a}^j)^\top \mathrm{Diag}(\sqrt{\mathbf{V}(t)}) d\mathbf{Z}(t) \right) \\ &= \frac{S^{i,j}(t)B^j(t)}{B^i(t)} (\mathbf{a}^i - \mathbf{a}^j)^\top \mathrm{Diag}(\sqrt{\mathbf{V}(t)}) d\mathbf{Z}^{\mathbb{Q}^i}(t). \end{aligned} \tag{17}$$

In the last line we implicitly defined the new Brownian motion vector $\mathbf{Z}^{\mathbb{Q}^i}(t)$ under the measure $\mathbb{Q}^i$ from the constraint of having a $\mathbb{Q}^i$-local martingale and by Girsanov theorem:

$$d\mathbf{Z}(t)^{\mathbb{Q}^i} = d\mathbf{Z}(t) + \mathrm{Diag}(\sqrt{\mathbf{V}(t)})\mathbf{a}^i dt, \quad i = 1, .., N. \tag{18}$$

If we denote $\mathbb{Q}^0$ the risk neutral measure associated with the universal numéraire, the Radon-Nikodym derivative corresponding to the change of measure from $\mathbb{Q}^0$ to $\mathbb{Q}^i$ reads

$$\frac{d\mathbb{Q}^i}{d\mathbb{Q}^0}|_t = \exp\left(-\int_0^t \left(\mathbf{a}^i\right)^\top \mathrm{Diag}(\sqrt{\mathbf{V}(s)})d\mathbf{Z}(s) - \frac{1}{2}\int_0^t \left(\mathbf{a}^i\right)^\top \mathrm{Diag}(\mathbf{V}(s))\mathbf{a}^i ds\right), \tag{19}$$

where we observe that the shift is performed only on the process $\mathbf{Z}(t)$.

The $\mathbb{Q}^i$ risk neutral dynamics of the exchange rate $S^{i,j}(t)$ becomes

$$dS^{i,j}(t) = S^{i,j}(t)\left((r^i - r^j)dt + (\mathbf{a}^i - \mathbf{a}^j)^\top \mathrm{Diag}(\sqrt{\mathbf{V}(t)})d\mathbf{Z}^{\mathbb{Q}^i}(t)\right), \tag{20}$$

as desired.

Given our assumption on the correlation structure in (5), we can write the following standard factorization under $\mathbb{Q}^0$

$$dW_k(t) = \rho_k dZ_k(t) + \sqrt{1-\rho_k^2}dZ_k^\perp(t), \quad k = 1, ..., d. \tag{21}$$

where $\mathbf{Z}^\perp(t)$ is a Brownian motion independent of $\mathbf{Z}(t)$. Hence the measure change has also an impact on the variance processes, via the correlations $\rho_k, k = 1, .., d$,

$$dW_k^{\mathbb{Q}^i}(t) = dW_k(t) + \rho_k\left(\mathbf{e}^k\right)^\top \mathrm{Diag}(\sqrt{\mathbf{V}(t)})\mathbf{a}^i dt. \tag{22}$$

The component of $dW_k(t)$ which is orthogonal to the spot driver $d\mathbf{Z}(t)$ is not affected by the measure change. This choice may seem arbitrary at first sight, but it turns out to be consistent with the market practice. More importantly, [Del Baño Rollin, 2008] shows that this assumption constitutes a sufficient condition ensuring that the foreign-domestic parity is satisfied. We finally obtain the dynamic equations under the new measure. With an appropriate redefinition of the CIR parameters

$$\begin{aligned}\rho_k^{\mathbb{Q}^i} &= \rho_k,\\ \kappa_k^{\mathbb{Q}^i} &= \kappa_k + \xi_k\rho_k a_k^i,\\ \theta_k^{\mathbb{Q}^i} &= \theta_k\frac{\kappa_k}{\kappa_k^{\mathbb{Q}^i}},\end{aligned}$$

we can recast the variance SDE in its original form

$$dV_k(t) = \kappa_k^{\mathbb{Q}^i}(\theta_k^{\mathbb{Q}^i} - V_k(t))dt + \xi_k\sqrt{V_k(t)}dW_k^{\mathbb{Q}^i}(t). \tag{23}$$

We can now show that the Girsanov theorem used in (18) has been correctly applied.

Proposition 2. *The exponential local martingale (19) is a true martingale, that is* $\mathbb{E}^{\mathbb{Q}^0}\left[\frac{d\mathbb{Q}^i}{d\mathbb{Q}^0}|_t\right] = 1$.

Proof. See the Appendix. □

In the Appendix we derive a proof of the previous result based on the Feller explosion test for diffusions as in [Wong and Heyde, 2004] and [Mijatović and Urusov, 2011]. In order to get a quick intuition, from (19) we can check that the process $\mathbf{V}$ has the same behavior at the boundaries 0 and $+\infty$ under both measures $\mathbb{Q}^0$ and $\mathbb{Q}^i$. In fact the dimension of the process $\mathbf{V}$ and the boundary behavior at infinity are the same (that is the Feller condition is unchanged and the probability of an explosion in finite time is zero). As a consequence, the Radon-Nikodym derivative defined through (19) is a (true) martingale, so that the Girsanov change of measure is allowed.

The invariance of the functional form of the model under measure change is an appealing feature of our model; other specifications of the stochastic volatility will almost surely break this symmetry. Financially, it makes sense to enforce mean reversion of the variance, other than mean explosion, yielding a condition on $\kappa_k^{\mathbb{Q}^i} > 0$ or conversely on the original model parameters κ_k, ξ_k, ρ_k, and a_k^i.

The inverse FX rate follows from Ito calculus

$$\begin{aligned}\frac{dS^{j,i}(t)}{S^{j,i}(t)} &= S^{i,j}(t)d\left(\frac{1}{S^{i,j}(t)}\right) \qquad (24)\\ &= [r^j - r^i + (\mathbf{a}^j - \mathbf{a}^i)^\top \mathrm{Diag}(\mathbf{V}(t))(\mathbf{a}^j - \mathbf{a}^i)]dt + (\mathbf{a}^j - \mathbf{a}^i)^\top \mathrm{Diag}(\sqrt{\mathbf{V}(t)})d\mathbf{Z}^{\mathbb{Q}^i}(t),\end{aligned}$$

which includes the self-quanto adjustment. Similarly, the SDE of a generic cross FX rate becomes

$$\begin{aligned}\frac{dS^{j,l}(t)}{S^{j,l}(t)} &= \frac{S^{i,j}(t)}{S^{i,l}(t)}d\left(\frac{S^{i,l}(t)}{S^{i,j}(t)}\right) \qquad (25)\\ &= [r^j - r^l + (\mathbf{a}^j - \mathbf{a}^l)^\top \mathrm{Diag}(\mathbf{V}(t))(\mathbf{a}^j - \mathbf{a}^i)]dt + (\mathbf{a}^j - \mathbf{a}^l)^\top \mathrm{Diag}(\sqrt{\mathbf{V}(t)})d\mathbf{Z}^{\mathbb{Q}^i}(t).\end{aligned}$$

The additional drift term is the quanto adjustment as described by the current model choice. By applying Girsanov theorem again, this time switching to the $\mathbb{Q}^j$ risk neutral measure, the term is removed while the CIR parameters become

$$\begin{aligned}\kappa_k^{\mathbb{Q}^j} &= \kappa_k^{\mathbb{Q}^i} + \rho_k \xi_k (a_k^j - a_k^i),\\ \theta_k^{\mathbb{Q}^j} &= \theta_k^{\mathbb{Q}^i}\frac{\kappa_k^{\mathbb{Q}^i}}{\kappa_k^{\mathbb{Q}^j}}, \qquad (26)\end{aligned}$$

together with the invariant $\rho_k^{\mathbb{Q}^j} = \rho_k^{\mathbb{Q}^i}$ and $\xi_k^{\mathbb{Q}^j} = \xi_k^{\mathbb{Q}^i}$. These are the fundamental transformation rules for the model parameters.

4 Option pricing

Together with the invariance of the model specification with respect to the numéraire choice, a second central feature of the model is the availability of a (semi)-analytical solution for *all* vanilla option prices. The pricing formula itself is independent of the option underlying, once we work under the risk neutral measure associated with one of the currencies in the option and the parameters are transformed via (26).

Let us consider a call option $C(S^{i,j}(t), K^{i,j}, \tau), i, j = 1, .., N, i \neq j$, on a generic FX rate $S^{i,j}(t) = \exp(x^{i,j}(t))$ with strike $K^{i,j}$, maturity T ($\tau = T - t$ is the time to maturity) and face equal to one unit of the foreign currency. We write for the CIR parameters $\kappa_k = \kappa_k^{\mathbb{Q}^i}, \theta_k = \theta_k^{\mathbb{Q}^i}$ and so on, implicitly assuming that they have been transformed via (26) in the i-th risk neutral measure $\mathbb{Q}^i$. Being an affine model, the (generalized) characteristic function conditioned on the initial values

$$\phi^{i,j}(\omega, t, \tau, x, \mathbf{V}) = \mathbb{E}_t^{\mathbb{Q}^i}[e^{\mathtt{i}\omega x^{i,j}(T)} | x^{i,j}(t) = x, \mathbf{V}(t) = \mathbf{V}] \tag{27}$$

can be derived analytically (here $\mathtt{i} = \sqrt{-1}$). Standard numerical integration methods can then be used to invert the Fourier transform to obtain the probability density at T or the vanilla price via integration against the payoff, with overall little computational effort. By applying standard arguments (see e.g. [Lewis, 2000], [Sepp, 2003]) the value of a call option can be expressed in terms of the integral of the product of the Fourier transform of the payoff and the generalized characteristic function of the log-asset price[1]:

$$C(S^{i,j}(t), K^{i,j}, \tau) = e^{-r^i \tau} \frac{1}{2\pi} \int_{\mathcal{Z}} \phi^{i,j}(-\mathtt{i}\lambda, t, \tau, x, \mathbf{V}) \Phi(\lambda) d\lambda, \tag{28}$$

where

$$\Phi(\lambda) = \int_{\mathcal{Z}} e^{\mathtt{i}\lambda x} \left(e^x - K^{i,j}\right)^+ dx$$

is the Fourier transform of the payoff function and $\mathcal{Z}$ denotes the strip of regularity of the payoff, that is the admissible domain where the integral in (28) is well defined. In other words, the pricing problem is essentially solved once the (conditional) characteristic function of the log-exchange rate is known. We recall the relationship between the characteristic function and the moment generating function. In what follows we will derive the moment generating function $G^{i,j}(\omega, t, \tau, x, \mathbf{V})$ (Laplace tranform) from which the characteristic function is easily derived via a rotation in the complex plane $\phi^{i,j}(\omega, t, \tau, x, \mathbf{V}) = G^{i,j}(\mathtt{i}\omega, t, \tau, x, \mathbf{V})$. It is therefore sufficient to determine the moment generating function, as in the following proposition:

Proposition 3. *In the Multi-Heston model the conditional Laplace transform of the log-exchange rate is given by:*

$$G^{i,j}(\omega, t, \tau, x, \mathbf{V}) = \exp\left[\omega x + \left(r^i - r^j\right)\omega(\tau) + \sum_{k=1}^{d} \left(A_k^{i,j}(\tau) + B_k^{i,j}(\tau) V_k\right)\right], \tag{29}$$

---

[1] Here we adopt the pricing method of [Lewis, 2000] who uses the characteristic function computed with a complex argument, also called generalized characteristic function. The complex argument ω typically belongs to a strip of regularity for the function $\phi^{i,j}$ in order to be able to integrate the payoff function. On the other hand, this method avoids the introduction of the damping integrating factor required by the methodology of [Carr and Madan, 1999].

where for $k = 1, .., d$*:*

$$A_k^{i,j}(\tau) = \frac{2\kappa_k\theta_k}{\xi_k^2} \log \frac{\lambda_k^+ - \lambda_k^-}{\lambda_k^+ e^{\lambda_k^-(\tau)} - \lambda_k^- e^{\lambda_k^+(\tau)}}; \tag{30}$$

$$B_k^{i,j}(\tau) = \frac{\left(\omega^2 - \omega\right)}{2} \left(a_k^i - a_k^j\right)^2 \frac{1 - e^{-\sqrt{\Delta_k}\tau}}{\lambda_k^+ e^{-\sqrt{\Delta_k}\tau} - \lambda_k^-}; \tag{31}$$

$$\Delta_k = \left(-\kappa_k + \omega\left(a_k^i - a_k^j\right)\rho_k\xi_k\right)^2 - \xi_k^2\left(\omega^2 - \omega\right)\left(a_k^i - a_k^j\right)^2; \tag{32}$$

$$\lambda_k^\pm = \frac{\left(-\kappa_k + \omega\left(a_k^i - a_k^j\right)\rho_k\xi_k\right) \pm \sqrt{\Delta_k}}{2}. \tag{33}$$

Proof. See Appendix. □

In summary the call price is known once the characteristic function $G^{i,j}$ is known explicitly, as in the present framework.

5 Expansions

As we will see in the sequel, the calibration of our model can be performed by relying on a standard non-linear least squares procedure, which will be employed to minimize the distance between the model implied volatilities and market ones. Model implied volatilities are extracted from the prices produced by the FFT routine. This procedure is quite demanding from a numerical point of view. An alternative approach consists in fitting implied volatilities via a simpler function, for example by looking at a possible relationship between the prices produced by the model, see (28), and the standard Black-Scholes formula for a suitable volatility. The next result states that it is possible to approximate the prices of options under the multi-Heston model, via a suitable expansion of the standard Black-Scholes formula and its derivatives. The proof, which is reported in the appendix, relies on arguments which may be found in [Lewis, 2000] and [Da Fonseca and Grasselli, 2011] (we drop all currency indices, it is intended that we are considering the (i, j) FX pair). Define $\tau = T - t$ and let us define the real deterministic functions $\mathcal{B}_k^{(0)}, \mathcal{B}_k^{(1)}, \mathcal{B}_k^{(2)}, \mathcal{B}_k^{(3)}, k = 1, .., d$ as

$$\mathcal{B}_k^{(0)}(\tau) = \left(a_k^i - a_k^j\right)^2 \frac{1 - e^{-\kappa_k\tau}}{\kappa_k}; \tag{34}$$

$$\mathcal{B}_k^{(1)}(\tau) = \left(a_k^i - a_k^j\right)^3 \rho_k\xi_k \left(\frac{1}{\kappa_k^2} - \frac{e^{-\kappa_k\tau}}{\kappa_k^2} - \frac{\tau e^{-\kappa_k\tau}}{\kappa_k}\right); \tag{35}$$

$$\mathcal{B}_k^{(2)}(\tau) = \left(a_k^i - a_k^j\right)^4 \frac{\xi_k^2}{2\kappa_k^2} \left(\frac{1 - e^{-2\kappa_k\tau}}{\kappa_k} - 2\tau e^{-\kappa_k\tau}\right); \tag{36}$$

$$\mathcal{B}_k^{(3)}(\tau) = \left(a_k^i - a_k^j\right)^4 \rho_k^2\xi_k^2 \left(\frac{1 - e^{-\kappa_k\tau}}{\kappa_k^3} - \frac{\tau e^{-\kappa_k\tau}}{\kappa_k^2} - \frac{\tau^2 e^{-\kappa_k\tau}}{2\kappa_k}\right) \tag{37}$$

and $\mathcal{A}_k^{(0)}, \mathcal{A}_k^{(1)}, \mathcal{A}_k^{(2)}, \mathcal{A}_k^{(3)}, k = 1, .., d$ as

$$\mathcal{A}_k^{(0)}(\tau) = \left(a_k^i - a_k^j\right)^2 \theta_k \left(\tau + \frac{e^{-\kappa_k \tau} - 1}{\kappa_k}\right); \tag{38}$$

$$\mathcal{A}_k^{(1)}(\tau) = \left(a_k^i - a_k^j\right)^3 \theta_k \rho_k \xi_k \left(\frac{\tau}{\kappa_k} + 2\frac{e^{-\kappa_k \tau} - 1}{\kappa_k^2} + \frac{\tau e^{-\kappa_k \tau}}{\kappa_k}\right); \tag{39}$$

$$\begin{aligned}\mathcal{A}_k^{(2)}(\tau) = \left(a_k^i - a_k^j\right)^4 \theta_k \rho_k^2 \xi_k^2 \Bigg(& \frac{\tau}{\kappa_k} + \frac{e^{-\kappa_k \tau} - 1}{\kappa_k^3} + \frac{\tau e^{-\kappa_k \tau}}{\kappa_k^2} \\ & - \frac{e^{-\kappa_k \tau} - 1}{\kappa_k^2} + \frac{\tau^2 e^{-\kappa_k \tau}}{2\kappa_k} - \frac{\tau e^{-\kappa_k \tau}}{\kappa_k} + \frac{e^{-\kappa_k \tau} - 1}{\kappa_k}\Bigg);\end{aligned} \tag{40}$$

$$\mathcal{A}_k^{(3)}(\tau) = \left(a_k^i - a_k^j\right)^4 \theta_k \rho_k^2 \xi_k^2 \left(\frac{\tau}{\kappa_k^2} + 3\frac{e^{-\kappa_k \tau} - 1}{\kappa_k^3} + 2\frac{\tau e^{-\kappa_k \tau}}{\kappa_k^2} + \frac{\tau^2 e^{-\kappa_k \tau}}{2\kappa_k}\right). \tag{41}$$

Finally, define the integrated variance as:

$$v = \sigma^2 \tau = \sum_{k=1}^{d} \left(\mathcal{A}_k^{(0)}(\tau) + \mathcal{B}_k^{(0)}(\tau) V_k\right). \tag{42}$$

Proposition 4. *Assume that all vol-of-vol parameters $\xi_k, k = 1, .., d$ have been scaled by the same factor $\alpha > 0$. Then the call price $C(S(t), K, \tau)$ in the Multi-factor Heston-based exchange model can be approximated in terms of the scale factor α by differentiating the Black Scholes formula $C_{\text{BS}}\left(S(t), K, \sigma, \tau\right)$ with respect to the log exchange rate $x(t) = \ln S(t)$ and the integrated variance $v = \sigma^2 \tau$:*

$$\begin{aligned} C(S(t), K, \tau) \approx\ & C_{\text{BS}}\left(S(t), K, \sigma, \tau\right) \\ & + \alpha \sum_{k=1}^{d} \left(\mathcal{A}_k^{(1)}(\tau) + \mathcal{B}_k^{(1)}(\tau) V_k\right) \partial_{xv}^2 C_{\text{BS}}\left(S(t), K, \sigma, \tau\right) \\ & + \alpha^2 \sum_{k=1}^{d} \left(\mathcal{A}_k^{(2)}(\tau) + \mathcal{B}_k^{(2)}(\tau) V_k\right) \partial_{vv}^2 C_{\text{BS}}\left(S(t), K, \sigma, \tau\right) \\ & + \alpha^2 \sum_{k=1}^{d} \left(\mathcal{A}_k^{(3)}(\tau) + \mathcal{B}_k^{(3)}(\tau) V_k\right) \partial_{xxv}^3 C_{\text{BS}}\left(S(t), K, \sigma, \tau\right) \\ & + \frac{\alpha^2}{2} \left[\sum_{k=1}^{d} \left(\mathcal{A}_k^{(1)}(\tau) + \mathcal{B}_k^{(1)}(\tau) V_k\right)\right]^2 \partial_{xxvv}^4 C_{\text{BS}}\left(S(t), K, \sigma, \tau\right). \end{aligned} \tag{43}$$

Proof. See Appendix. ☐

We can now state another formula, which does not involve the computation of option prices and constitutes an approximation of the implied volatility surface for a short time to maturity. This formula may constitute a useful alternative in order to get a quicker calibration for short maturities. The proof is again provided in detail in the Appendix.

Proposition 5. *For a short time to maturity the implied volatility expansion in terms of the vol-of-vol scale factor α in the multifactor Heston-based exchange model is given by:*

$$\sigma_{\mathrm{imp}}^2 \approx \sigma_0^2 + \alpha \left(\sum_{k=1}^{d} \frac{\rho_k \xi_k}{2} \left(a_k^i - a_k^j \right)^4 V_k \right) \frac{m_f}{\sigma_0^2}$$
$$+ \alpha^2 \frac{m_f^2}{12 \left(\sigma_0^2\right)^2} \left[\sum_{k=1}^{d} \left(1 + 2\rho_k^2\right) \xi_k^2 \left(a_k^i - a_k^j \right)^4 V_k - \frac{15}{4\sigma_0^2} \left(\sum_{k=1}^{d} \rho_k \xi_k \left(a_k^i - a_k^j \right)^3 V_k \right)^2 \right],$$

where $\sigma_0^2 = \left(\mathbf{a}^i - \mathbf{a}^j\right)^\top \mathrm{Diag}(\mathbf{V}) \left(\mathbf{a}^i - \mathbf{a}^j\right)$ *and* $m_f = \log\left(\frac{S^{i,j} e^{(r^i - r^j)\tau}}{K^{i,j}}\right)$ *denotes the forward log-moneyness.*

Proof. See Appendix. ☐

6 Simultaneous calibration of the USD/EUR/JPY triangle

6.1 Setup

In this section we show an example of simultaneous calibration to three market volatility surfaces of options: we consider the implied volatility surfaces for USD/EUR, USD/JPY and EUR/JPY as observed in the FX market on a typical day (data from 23rd July 2010), that is $N = 3$ with $i =$ USD; EUR; JPY. The volatility sample includes expiry dates ranging from 3 days to 5 years. The quotes follow the standard Delta quoting conversion in the FX option market, we have quotes on DN, 25 Delta, 15 Delta, and 10 Delta[2].

We try to fit simultaneously the three volatility surfaces using two stochastic drivers, $d = 2$. This choice yields a total number of parameters $N_P = 16$, comparable to the number of parameters in 3 independent Heston models (15 parameters). This choice should not lead to overfitting instabilities. We work under the USD risk neutral measure to derive the option prices of the pairs EUR/USD and USD/JPY and the EUR measure for the EUR/JPY options, using (28). We calibrate the CIR parameters in the USD measure $\kappa_k^{\mathrm{USD}}, \theta_k^{\mathrm{USD}}, \xi_k^{\mathrm{USD}}, \rho_k^{\mathrm{USD}},\ k = 1, 2$. The parameters for the EUR/JPY are transformed to the EUR measure through Eqs. (26) and the invariance property of correlation and vol-of-vol parameters.

The calibration is done via a standard non-linear least-squares optimizer that minimizes the total calibration error in terms of the difference between calibrated and target implied volatilities

---

[2] It is important to stress that in the forex market implied volatilities surfaces are expressed in terms of maturity and Delta (see e.g. [Wystup and Reiswich, 2010], [Clark, 2011]): the market practice is to quote volatilities for strangles and risk reversals which can then be employed to reconstruct a whole surface of implied volatilities via an interpolation method (see e.g. [Wystup and Reiswich, 2010], [Wystup, 2006], [Clark, 2011]). Once we have the quotes in terms of Delta, to perform the calibration we have to convert Deltas into strike prices. The procedure can be found e.g. in [Beneder and Elkenbracht-Huizing, 2003].

$$\mathrm{Err} = \sum_{n} \left(\sigma^{\mathrm{imp}}_{n,\mathrm{market}} - \sigma^{\mathrm{imp}}_{n,\mathrm{model}} \right)^2 . \tag{44}$$

The use of a norm in price should be avoided as the numerical range for option prices may be large, thus introducing a bias in the optimization (for a more detailed discussion, see [Da Fonseca and Grasselli, 2011]).

6.2 Calibration results

In Table (1) we report the result of the calibration of the model. We performed the optimization considering different sets of expiries. The expiries considered in the largest sample are the following: 1, 2, 3, 6, 9 months and 1 year. The result for this particular choice of expiries is reported on the first column on the left. Then we repeated the experiment by excluding the largest expiry, 1 year. The result is reported in the second column. We proceed in this way by excluding more and more expiries. The smallest sample is reported in the last column and considers only options expyring in 1 and 2 months.

In Figs. 1, 2 and 3 we plot the market implied volatilities against those produced by the model. The plots refer to the largest sample in Table 1. Market volatilities are denoted by crosses, model volatilities are denoted by circles. The model yields a satisfactory fit of the market points. We are not aware of any other stochastic volatility model that can achieve a simultaneous calibration of a three-currency triangle with this accuracy.

The plots for the calibration on the sub-samples are completely analogous.

6.3 Parameters stability tests

In this subsection we comment on the stability of the parameters via two different types of analysis. We first measure the impact on the parameters resulting from the calibration procedure. Secondly, we fit the model parameters to a certain sample and then use these parameters to price an option which is not included in the sample. If the out-of-sample prices are close to the market, the model gives a reasonable description of the joint underlying FX rates dynamics. Moreover, the calibration can be done on a limited set of expiries, reducing the computation effort of the optimizer.

As far as the first analysis is concerned, we show in Table 2 the relative variations computed with respect to the largest sample. With the exception of κ_1 we can see that there is a good degree of stability of the parameters across the sub-samples. Since κ_1 is the only value which seems to fluctuate significantly, we perform also a second calibration experiment, where we fix $\kappa_k = 1, k = 1, 2$. The results of this experiment are outlined in Table 3. The relative variation of the parameters can be found in Table 4. We notice that with this choice we get a good degree of stability, the most relevant fluctuation is now around 20% for θ_1[3].

---

[3] We do not report, for the sake of brevity, the volatility surfaces arising from this last experiment, but the quality of the fit is the same as before.

Let us now turn our attention to the out-of-sample exercise. In Tables 6, 7, 8 and 9 we show the difference between the market and the out-of-sample volatility for all sub-samples. The differences are always well below one volatility point, hence satisfactory.

6.4 Feller condition

It is well known, see e.g. [Feller, 1951, Andersen and Piterbarg, 2007], that for square root processes 0 represents an attainable state when the Feller condition is not satisfied, that is when $2\kappa_k\theta_k < \xi_k^2$. In our modelling framework we have two volatility factors, hence we can perform the check for each factor. In Table 5 we report the quantity $F_k = 2\kappa_k\theta_k - \xi_k^2, k = 1, 2$. We observe violations of the Feller condition, which constitutes a well-known fact in the FX derivative practice, shared with the standard one-dimensional Heston model, see [Clark, 2011].

6.5 Moment explosions

Another well established fact is that stochastic volatility models often suffer of pathological moment explosions which might often impact the stability of the pricing tools, see e.g. [Andersen and Piterbarg, 2007], [Keller-Ressel, 2011] and [Glasserman and Kim, 2011]. The model dynamics might lead to the explosion of moments, which become infinite in finite time.

Qualitatively, the present model shares with the Heston model the same type of singularities. Let us define the explosion time of the n-th moment as:

$$T_\star(n) = \sup\left\{t > 0 : \ \mathbb{E}\left[(S^{i,j}(t))^n\right] < \infty\right\}. \tag{45}$$

In our 2-Heston model, the n-th moment $m_n(t) = \mathbb{E}\left[\left(S^{i,j}(t)\right)^n\right]$ is computed by (3) as follows:

$$\begin{aligned} m_n(t) =& G^{i,j}(n, 0, t, x, \mathbf{V}) && (46)\\ =& (S^{i,j}(0))^n e^{n(r^i - r^j)t} \exp\left\{A_1^{i,j}(t) + B_1^{i,j}(t)V_1(0)\right\} && (47)\\ & . \exp\left\{A_2^{i,j}(t) + B_2^{i,j}(t)V_2(0)\right\} && (48) \end{aligned}$$

where the functions $A_k^{i,j}(t), B_k^{i,j}(t)$ are given in Proposition 3 with $\omega = n$. Hence, the moments can be decomposed in a product of one-dimensional moment generating functions. As a result, the moment explosion properties follow directly from the known results of the one-dimensional Heston model.

In complete analogy with [Keller-Ressel, 2011] (Section 6.1), from the Riccati ODE (60) for each factor $k = 1, 2$, we define the quantities $\Delta_k(n)$ and $\chi_k(n)$ as follows:

$$\Delta_k(n) = \left(\kappa_k - \omega\left(a_k^i - a_k^j\right)\rho_k\xi_k\right)^2 - (\omega^2 - \omega)\left(a_k^i - a_k^j\right)^2; \tag{49}$$

$$\chi_k(n) = -\kappa_k + \omega\left(a_k^i - a_k^j\right)\rho_k\xi_k. \tag{50}$$

We can then apply the moment explosion formula and obtain the following

Proposition 6. *In the multi-Heston model, $T_\star(n)$ is given by:*

1. $T_\star(n) = +\infty$, *if* $\Delta_k(n) \geq 0, \forall k = 1, 2$*;*
2. $T_\star(n) = \inf_k \left\{ \frac{2}{\sqrt{-\Delta_k(n)}} \left(\arctan\left(\frac{\sqrt{-\Delta_k(n)}}{\chi_k(n)} \right) + \pi \mathbf{1}_{\chi_k(n)<0} \right) \right\}$, *if* $\Delta_k(n) < 0$*, for some* $k = 1, 2$*.*

Then we can easily calculate the time of moment explosion for all currency pairs. In Table 14 we consider moments up to order 5.

6.6 Implied risk-neutral distribution

As a result of our calibration procedure, we have a set of model parameters allowing us to compute option prices which are in line with market data. The implied risk neutral probability densities of the different FX rates can be derived from option prices (cfr e.g. [Breeden and Litzenberger, 1978])

$$\varphi_t(S) = e^{r_i(T-t)} \left. \frac{\partial^2 C(S(t), K, T)}{\partial K^2} \right|_{K=S} . \tag{51}$$

The second derivative is approximated given a grid of option prices. We show the results in Figs. 4, 5 and 6. Notice that we plot the raw distribution resulting from prices, thus some numerical treatment is required in order to get a smooth distribution. All distributions feature asymmetry and leptokurtosis, features that are standard for returns in financial series.

7 Conclusions

We have introduced a new multi-factor stochastic volatility Heston-based model that can provide an accurate joint description of multiple FX vanilla options across different currency pairs. The emphasis in the model specification has been in the preservation of the specific symmetries of FX markets. Differently from other asset classes, appropriate multiplications/divisions and inversions of FX rates are still FX rates. Having a model that is functionally invariant with respect to these operations has immediate benefits: the calibrations are by construction universal, i.e., independent on the choice of the risk-free rate of the investor, leading to consistent prices and risk-sensitivities for multi-dimensional exotic options.

The choice of the CIR dynamics for the stochastic variance is instrumental in achieving this symmetry. We have indeed proven that our model is invariant with respect to the choice of the numéraire once the model parameters are appropriately transformed. The model is always of affine-type independently on which currency is used as risk free, leading to semi-analytical expression for all vanilla options between *any* of two currencies. This property is crucial when it comes to calibrating the model. In a standard global optimization algorithm we can consider together vanilla options in all currency pairs and achieve a simultaneous fit to the different volatility surfaces with reasonable computational effort.

The model shares naturally several stylized facts with the Heston model. The Feller condition is often violated when fitting the model to FX volatility surfaces, a common observation in the practice. Moreover, higher moments of the spot distribution explode at finite time; a property that might lead to complications/instabilities in standard numerical pricing routines. Finally, like any pure stochastic volatility model, our model cannot be expected to deliver a perfect calibration of the vanilla surfaces across all Deltas and tenors, especially in the short end.

Having said that, the main result of the paper is a promising joint calibration of the model to the implied volatilities smile of the EUR/USD/JPY FX triangle. The fit remains satisfactory across the currency pairs, Deltas and tenors which were considered. Several in- and out-of-sample calibration studies in fact have proven the robustness of the calibration, especially once the mean reversion speed κ has been fixed. Asymptotic expansions of the implied volatility surface are also included as they shed light on the meaning of the different model parameters and can help speeding up the calibration procedure.

The price to pay in order to obtain a consistent simultaneous calibration to all volatilities surfaces is that the instantaneous volatilities of the currency pairs do not have single dedicated drivers. Their dynamics is rather brought about by a linear combination of several hidden stochastic factors. As in any principal component analysis, it is not easy to assign a financial meaning to each model parameter. As this study has shown, this appealing feature has most likely to be traded away in order to capture the complex phenomenology of the present global and widely interconnected FX markets.

8 Appendix A: Proofs

8.1 Proof of Proposition (2)

We will apply Theorem 2.1 from [Mijatović and Urusov, 2011]: using their notation we have $Y_k = V_k$ and $b_k(x) = -\rho_k x_k^{1/2} a_k^i$, where we recall that by independency of the V_k processes the Radon-Nykodim derivative splits in a product and we can use a separability argument.

If the Feller condition holds, that is when $2\kappa_k\theta_k \geq \xi_k^2$, then conditions a) and c) in Theorem 2.1 of [Mijatović and Urusov, 2011] hold, as from (23) we note that the boundary behavior of V_k is the same under both $\mathbb{Q}^0$ and $\mathbb{Q}^i$.

Suppose now that the Feller condition is violated. Condition a) still holds while condition c) does not, but the boundary $l = 0$ is good. To see this let us compute the functions $\rho_k(x), s_k(x)$ (given by formulae (16),(18) in [Mijatović and Urusov, 2011]) in our framework:

$$\rho_k(x) = \alpha x^{-\frac{2\kappa_k\theta_k}{\xi_k^2}} \exp(\frac{2\kappa_k x}{\xi_k^2}) \,,$$

where α denotes a positive constant, and

$$s_k(x) = \int_c^x \rho(y)dy = \alpha \int_c^x y^{-\frac{2\kappa_k\theta_k}{\xi_k^2}} \exp(\frac{2\kappa_k y}{\xi_k^2})dy \,,$$

where c denotes another arbitrary constant. We can now confirm using (26) in [Mijatović and Urusov, 2011], that 0 is good: in fact we have $s_k(0) > -\infty$ (by the assumption $2\kappa_k\theta_k < \xi_k^2$) and the function

$$\frac{(s_k(x)-s_k(0))b_k^2(x)}{\rho_k(x)\sigma_k^2(x)} = \alpha(s_k(x)-s_k(0))x^{\frac{2\kappa_k\theta_k}{\xi_k^2}}\exp(\frac{2\kappa_k x}{\xi_k^2})$$

is locally integrable around 0 since $s_k(x)$ behaves like $x^{-\frac{2\kappa_k\theta_k}{\xi_k^2}+1}$. Hence (26) holds and it follows that the Radon-Nykodim derivative (19) is a true martingale.

8.2 Proof of Proposition (3)

Recall that $\phi\left(\omega,t,\tau,x,\mathbf{V}\right) = G(\mathrm{i}\omega,t,\tau,x,\mathbf{V})$, with $x^{i,j}(t) = \log S^{i,j}(t)$. The functions ϕ, G represent resp. the characteristic function and the moment generating function of the log-exchange rate. In order to determine these quantities, we first need to write the PDE satisfied by G. First of all we write down the dynamics of $x = x^{i,j}$:

$$\begin{aligned} dx(t) &= \left(\left(r^i - r^j\right) - \frac{1}{2}(\mathbf{a}^i - \mathbf{a}^j)^\top \mathrm{Diag}\left(\mathbf{V}(t)\right)\left(\mathbf{a}^i - \mathbf{a}^j\right)\right)dt \\ &\quad + \left(\mathbf{a}^i - \mathbf{a}^j\right)^\top \mathrm{Diag}\left(\sqrt{\mathbf{V}(t)}\right) d\mathbf{Z}^{\mathbb{Q}^i}(t). \end{aligned} \tag{52}$$

We also compute the following covariation terms for $k = 1,..,d$:

$$\begin{aligned} d\left\langle x, V_k\right\rangle_t &= \left\langle \left(\mathbf{a}^i - \mathbf{a}^j\right)^\top \mathrm{Diag}\left(\sqrt{\mathbf{V}}\right) d\mathbf{Z}^{\mathbb{Q}^i}, \xi_k\sqrt{V_k}\rho_k dZ_k^{\mathbb{Q}^i}\right\rangle_t \\ &= \left\langle \left(a_k^i - a_k^j\right)\sqrt{V_k}dZ_k^{\mathbb{Q}^i}, \xi_k\sqrt{V_k}\rho_k dZ_k^{\mathbb{Q}^i}\right\rangle_t \\ &= \left(a_k^i - a_k^j\right)V_k(t)\xi_k\rho_k dt. \end{aligned} \tag{53}$$

The Laplace transform G solves the following backward Kolmogorov equation ([Karatzas and Shreve, 1991]):

$$\begin{aligned} &\frac{\partial G}{\partial t} + \frac{1}{2}\frac{\partial^2 G}{\partial x^2}\left(\mathbf{a}^i - \mathbf{a}^j\right)^\top \mathrm{Diag}\left(\mathbf{V}\right)\left(\mathbf{a}^i - \mathbf{a}^j\right) \\ &\sum_{k=1}^d \frac{\partial^2 G}{\partial x \partial V_k}\left(a_k^i - a_k^j\right)V_k\xi_k\rho_k + \frac{1}{2}\sum_{k=1}^d \frac{\partial^2 G}{\partial V_k^2}\xi_k^2 V_k \\ &\left(\left(r^i - r^j\right) - \frac{1}{2}\left(\mathbf{a}^i - \mathbf{a}^j\right)^\top \mathrm{Diag}\left(\mathbf{V}\right)\left(\mathbf{a}^i - \mathbf{a}^j\right)\right)\frac{\partial G}{\partial x} \\ &+ \sum_{k=1}^d \frac{\partial G}{\partial V_k}\kappa_k\left(\theta_k - V_k\right) = 0 \end{aligned} \tag{54}$$

with terminal condition $G\left(\omega,T,0,x,\mathbf{V}\right) = e^{\omega x}$ with $\omega \in \mathbb{R}$. In order to solve this problem we look for an exponential affine solution of the form:

$$G\left(\omega,t,\tau,x,\mathbf{V}\right) = \exp\left(A(t,T) + \sum_{k=1}^d B_k(t,T)V_k + C(t,T)x\right), \tag{55}$$

for some deterministic functions A, B_k, C that may depend on both t, T. Upon substitution of the guess and recognition of the terms we obtain the following system of $d+2$ ODE's:

$$\frac{\partial A}{\partial t}+\sum_{k=1}^{d} B_k(t,T)\kappa_k\theta_k+\left(r^i-r^j\right)C(t,T)=0; \tag{56}$$

$$\begin{aligned}&\frac{\partial B_k}{\partial t}+\frac{1}{2}C^2(t,T)\left(a_k^i-a_k^j\right)^2+C(t,T)B_k(t,T)\left(a_k^i-a_k^j\right)\rho_k\xi_k\\&+\frac{1}{2}B_k^2(t,T)\xi_k^2-\frac{1}{2}\left(a_k^i-a_k^j\right)^2C(t,T)-B_k(t,T)\kappa_k=0;\end{aligned} \tag{57}$$

$$\frac{\partial C}{\partial t}=0, \tag{58}$$

with terminal conditions: $A(T,T)=0,\quad B_k(T,T)=0,\quad C(T,T)=\omega$ for $k=1,..,d$. From (58) and its terminal condition, we deduce that $C(t,T)=\omega$ for $t\in[0,T]$, so we can rewrite the system as follows:

$$\frac{\partial A}{\partial t}+\sum_{k=1}^{d}\kappa_k\theta_k B_k(t,T)+\left(r^i-r^j\right)\omega=0; \tag{59}$$

$$\begin{aligned}&\frac{\partial B_k}{\partial t}+\frac{1}{2}B_k^2(t,T)\xi_k^2+\left(-\kappa_k+\omega\left(a_k^i-a_k^j\right)\rho_k\xi_k\right)B_k(t,T)\\&+\frac{\omega^2-\omega}{2}\left(a_k^i-a_k^j\right)^2=0,\quad k=1,..,d.\end{aligned} \tag{60}$$

Now for $d=1,..,d$ we assume that $B_k(t,T)$ can be written by means of a function $E_k(t,T)$ and set:

$$B_k(t,T)=\frac{\frac{\partial}{\partial t}E_k(t,T)}{\frac{\xi_k^2}{2}E_k(t,T)}, \tag{61}$$

then the solution for (60) is:

$$B_k(t,T)=\frac{\left(\omega^2-\omega\right)}{2}\left(a_k^i-a_k^j\right)^2\frac{1-e^{-\sqrt{\Delta_k}(T-t)}}{\lambda_k^+e^{-\sqrt{\Delta_k}(T-t)}-\lambda_k^-}, \tag{62}$$

with

$$\Delta_k=\left(-\kappa_k+\omega\left(a_k^i-a_k^j\right)\rho_k\xi_k\right)^2-\xi_k^2\left(\omega^2-\omega\right)\left(a_k^i-a_k^j\right)^2 \tag{63}$$

$$\lambda_k^{\pm}=\frac{\left(-\kappa_k+\omega\left(a_k^i-a_k^j\right)\rho_k\xi_k\right)\pm\sqrt{\Delta_k}}{2}. \tag{64}$$

Equipped with the solution for $B_k(t,T)$ we can now compute $A(t,T)$ as follows:

$$\begin{aligned}A(T,T)-A(t,T)&=\int_t^T\frac{\partial}{\partial u}A(u,T)du\\A(t,T)&=\int_t^T\sum_{k=1}^{d}\kappa_k\theta_k B_k(u,T)+\left(r^i-r^j\right)\omega du\\&=\left(r^i-r^j\right)\omega(T-t)+\sum_{k=1}^{d}\kappa_k\theta_k\int_t^T B_k(u,T)du\\&=\left(r^i-r^j\right)\omega(T-t)+\sum_{k=1}^{d}\frac{2\kappa_k\theta_k}{\xi_k^2}\int_t^T\frac{\frac{\partial}{\partial t}E_k(t,T)}{E_k(t,T)}du,\end{aligned} \tag{65}$$

which implies that the solution for $A(t,T)$ is

$$\begin{aligned}
A(t,T) &= \left(r^i - r^j\right)\omega(T-t) + \sum_{k=1}^{d} \frac{2\kappa_k\theta_k}{\xi_k^2} \log \frac{\lambda_k^+ - \lambda_k^-}{\lambda_k^+ e^{\lambda_k^-(T-t)} - \lambda_k^- e^{\lambda_k^+(T-t)}} \\
&= \left(r^i - r^j\right)\omega(T-t) + \sum_{k=1}^{d} A_k(t,T), \qquad (66)
\end{aligned}$$

where the functions $A_k(t,T)$ are implicitly defined by the last equality for $d = 1,..,d$. Now we obtain the statement of the proposition once we replace $B_k^{i,j}(\tau) = B_k(t,T), A_k^{i,j}(\tau) = A_k(t,T)$ with $\tau = T - t$.

8.3 Proof of Proposition (4)

The starting point is given by the Riccati ODE (60) expressed in terms of time-to-maturity $\tau = T - t$ and perturbed by introducing the vol-of-vol scale parameter α:

$$\begin{aligned}
\frac{\partial B_k}{\partial \tau} &= \frac{1}{2}B_k^2(\tau)\alpha^2\xi_k^2 + \left(-\kappa_k + \omega\left(a_k^i - a_k^j\right)\rho_k\alpha\xi_k\right)B_k(\tau) \\
&+ \frac{\omega^2-\omega}{2}\left(a_k^i - a_k^j\right)^2, \quad k = 1,..,d. \qquad (67)
\end{aligned}$$

We consider the following expansion in terms of α: $B_k(\tau) = B_{k,0}(\tau) + \alpha B_{k,1}(\tau) + \alpha^2 B_{k,2}(\tau)$. By plugging in the expansion and upon recognition of terms we obtain the following system of ODE's:

$$\begin{aligned}
\frac{\partial B_{k,0}}{\partial \tau} &= -\kappa_k B_{k,0}(\tau) + \frac{\omega^2-\omega}{2}\left(a_k^i - a_k^j\right)^2; \qquad (68) \\
\frac{\partial B_{k,1}}{\partial \tau} &= -\kappa_k B_{k,1}(\tau) + \omega\left(a_k^i - a_k^j\right)\rho_k\xi_k B_{k,0}(\tau); \qquad (69) \\
\frac{\partial B_{k,2}}{\partial \tau} &= -\kappa_k B_{k,2}(\tau) + \omega\left(a_k^i - a_k^j\right)\rho_k\xi_k B_{k,1}(\tau) + \frac{1}{2}B_{k,0}^2(\tau)\xi_k^2. \qquad (70)
\end{aligned}$$

If we denote $\gamma := \frac{\omega^2-\omega}{2}$ then the solutions are easily computed as:

$$\begin{aligned}
B_{k,0}(\tau) &= \underbrace{B_{k,0}(0)}_{=0} e^{-\kappa_k\tau} + e^{-\kappa_k\tau}\int_0^\tau e^{\kappa_k u}\gamma\left(a_k^i - a_k^j\right)^2 du \\
&= \gamma\mathcal{B}_k^{(0)}(\tau); \qquad (71) \\
B_{k,1}(\tau) &= \underbrace{B_{k,1}(0)}_{=0} e^{-\kappa_k\tau} + e^{-\kappa_k\tau}\int_0^\tau e^{\kappa_k u}\omega\left(a_k^i - a_k^j\right)\rho_k\xi_k\gamma\mathcal{B}_k^{(0)}(u)du \\
&= \omega\gamma\mathcal{B}_k^{(1)}(\tau); \qquad (72) \\
B_{k,2}(\tau) &= \underbrace{B_{k,2}(0)}_{=0} e^{-\kappa_k\tau} + e^{-\kappa_k\tau}\int_0^\tau e^{\kappa_k u}\omega^2\gamma\left(a_k^i - a_k^j\right)\rho_k\xi_k\mathcal{B}_k^{(1)}(u)du \\
&+ e^{-\kappa_k\tau}\int_0^\tau e^{\kappa_k u}\gamma\frac{\xi_k^2}{2}\left(\mathcal{B}_k^{(0)}(u)\right)^2 du \\
&= \omega^2\gamma\mathcal{B}_k^{(3)}(\tau) + \gamma^2\mathcal{B}_k^{(2)}(\tau). \qquad (73)
\end{aligned}$$

Then we can write the function $B_k(\tau)$ as follows:

$$B_k(\tau) = \gamma\mathcal{B}_k^{(0)}(\tau) + \alpha\omega\gamma\mathcal{B}_k^{(1)}(\tau) + \alpha^2\left(\omega^2\gamma\mathcal{B}_k^{(3)}(\tau) + \gamma^2\mathcal{B}_k^{(2)}(\tau)\right). \tag{74}$$

A direct substitution of (74) into (59) allows us to express the function $A(\tau)$:

$$\begin{aligned}
A(\tau) &= \omega\left(r^i - r^j\right)\tau + \sum_{k=1}^{d}\kappa_k\theta_k\int_0^\tau B_k(u)du \\
&= \omega\left(r^i - r^j\right)\tau + \gamma\sum_{k=1}^{d}\underbrace{\kappa_k\theta_k\int_0^\tau \mathcal{B}_k^{(0)}(u)du}_{:=\mathcal{A}_k^{(0)}(\tau)} + \omega\gamma\alpha\sum_{k=1}^{d}\underbrace{\kappa_k\theta_k\int_0^\tau \mathcal{B}_k^{(1)}(u)du}_{:=\mathcal{A}_k^{(1)}(\tau)} \\
&+ \omega^2\gamma\alpha^2\sum_{k=1}^{d}\underbrace{\kappa_k\theta_k\int_0^\tau \mathcal{B}_k^{(3)}(u)du}_{:=\mathcal{A}_k^{(3)}(\tau)} + \alpha^2\gamma^2\sum_{k=1}^{d}\underbrace{\kappa_k\theta_k\int_0^\tau \mathcal{B}_k^{(2)}(u)du}_{:=\mathcal{A}_k^{(2)}(\tau)}.
\end{aligned} \tag{75}$$

We consider then the price in terms of Fourier transform as in (28) by replacing the argument $\omega = \mathtt{i}\lambda$. A Taylor-McLaurin expansion w.r.t. α gives the following:

$$\begin{aligned}
C(S(t),K,\tau) &\approx \frac{e^{-r^i\tau}}{2\pi}\int_{\mathcal{Z}} e^{\mathtt{i}\lambda\left(r^i-r^j\right)\tau+\mathtt{i}\lambda x+\gamma\sum_{k=1}^{d}\left(\mathcal{A}_k^{(0)}(\tau)+\mathcal{B}_k^{(0)}(\tau)V_k\right)}\Phi(\lambda)d\lambda \\
&+ \alpha\sum_{k=1}^{d}\left(\mathcal{A}_k^{(1)}(\tau)+\mathcal{B}_k^{(1)}(\tau)V_k\right) \\
&\times \frac{e^{-r^i\tau}}{2\pi}\int_{\mathcal{Z}} \gamma\mathtt{i}\lambda e^{\mathtt{i}\lambda\left(r^i-r^j\right)\tau+\mathtt{i}\lambda x+\gamma\sum_{k=1}^{d}\left(\mathcal{A}_k^{(0)}(\tau)+\mathcal{B}_k^{(0)}(\tau)V_k\right)}\Phi(\lambda)d\lambda \\
&+ \alpha^2\sum_{k=1}^{d}\left(\mathcal{A}_k^{(2)}(\tau)+\mathcal{B}_k^{(2)}(\tau)V_k\right) \\
&\times \frac{e^{-r^i\tau}}{2\pi}\int_{\mathcal{Z}} \gamma^2 e^{\mathtt{i}\lambda\left(r^i-r^j\right)\tau+\mathtt{i}\lambda x+\gamma\sum_{k=1}^{d}\left(\mathcal{A}_k^{(0)}(\tau)+\mathcal{B}_k^{(0)}(\tau)V_k\right)}\Phi(\lambda)d\lambda \\
&+ \alpha^2\sum_{k=1}^{d}\left(\mathcal{A}_k^{(3)}(\tau)+\mathcal{B}_k^{(3)}(\tau)V_k\right) \\
&\times \frac{e^{-r^i\tau}}{2\pi}\int_{\mathcal{Z}} \gamma\mathtt{i}\lambda^2 e^{\mathtt{i}\lambda\left(r^i-r^j\right)\tau+\mathtt{i}\lambda x+\gamma\sum_{k=1}^{d}\left(\mathcal{A}_k^{(0)}(\tau)+\mathcal{B}_k^{(0)}(\tau)V_k\right)}\Phi(\lambda)d\lambda \\
&+ \frac{\alpha^2}{2}\left[\sum_{k=1}^{d}\left(\mathcal{A}_k^{(1)}(\tau)+\mathcal{B}_k^{(1)}(\tau)V_k\right)\right]^2 \\
&\times \frac{e^{-r^i\tau}}{2\pi}\int_{\mathcal{Z}} \gamma^2\mathtt{i}\lambda^2 e^{\mathtt{i}\lambda\left(r^i-r^j\right)\tau+\mathtt{i}\lambda x+\gamma\sum_{k=1}^{d}\left(\mathcal{A}_k^{(0)}(\tau)+\mathcal{B}_k^{(0)}(\tau)V_k\right)}\Phi(\lambda)d\lambda.
\end{aligned} \tag{76}$$

Recall now from (42) the definition of the integrated Black-Scholes variance. In the previous formula, in the first term on the right hand side, we recognise the

Black-Scholes price in terms of the characteristic function when the integrated variance is $v = \sigma^2\tau$:

$$C_{\mathrm{BS}}\left(S(t), K, \sigma, \tau\right) = \frac{e^{-r^i\tau}}{2\pi} \int_{\mathcal{Z}} e^{\mathtt{i}\lambda\left(r^i - r^j\right)\tau + \mathtt{i}\lambda x + \frac{(\mathtt{i}\lambda)^2 - \mathtt{i}\lambda}{2} v} \Phi(\lambda) d\lambda, \tag{77}$$

so that the price expansion is of the form:

$$\begin{aligned} C(S(t), K, \tau) \approx{} & C_{\mathrm{BS}}\left(S(t), K, \sigma, \tau\right) \\ & + \alpha \sum_{k=1}^{d} \left(\mathcal{A}_k^{(1)}(\tau) + \mathcal{B}_k^{(1)}(\tau) V_k\right) \partial_{xv}^2 C_{\mathrm{BS}}\left(S(t), K, \sigma, \tau\right) \\ & + \alpha^2 \sum_{k=1}^{d} \left(\mathcal{A}_k^{(2)}(\tau) + \mathcal{B}_k^{(2)}(\tau) V_k\right) \partial_{vv}^2 C_{\mathrm{BS}}\left(S(t), K, \sigma, \tau\right) \\ & + \alpha^2 \sum_{k=1}^{d} \left(\mathcal{A}_k^{(3)}(\tau) + \mathcal{B}_k^{(3)}(\tau) V_k\right) \partial_{xxv}^3 C_{\mathrm{BS}}\left(S(t), K, \sigma, \tau\right) \\ & + \frac{\alpha^2}{2} \left[\sum_{k=1}^{d} \left(\mathcal{A}_k^{(1)}(\tau) + \mathcal{B}_k^{(1)}(\tau) V_k\right)\right]^2 \partial_{xxvv}^4 C_{\mathrm{BS}}\left(S(t), K, \sigma, \tau\right). \end{aligned} \tag{78}$$

From the previous expression we can deduce the relation defining the deterministic functions $\mathcal{B}_k^{(h)}, \mathcal{A}_k^{(h)},\ h = 0, ..., 3.$

$$\mathcal{B}_k^{(0)}(\tau) = \left(a_k^i - a_k^j\right)^2 \frac{1 - e^{-\kappa_k\tau}}{\kappa_k}; \tag{79}$$

$$\mathcal{B}_k^{(1)}(\tau) = \left(a_k^i - a_k^j\right) \rho_k \xi_k e^{-\kappa_k\tau} \int_0^\tau e^{\kappa_k u} \mathcal{B}_k^{(0)}(u) du; \tag{80}$$

$$\mathcal{B}_k^{(2)}(\tau) = \frac{\xi_k^2}{2\kappa_k} e^{-\kappa_k\tau} \int_0^\tau e^{\kappa_k u} \left(\mathcal{B}_k^{(0)}(u)\right)^2 du; \tag{81}$$

$$\mathcal{B}_k^{(3)}(\tau) = \left(a_k^i - a_k^j\right) \rho_k \xi_k e^{-\kappa_k\tau} \int_0^\tau e^{\kappa_k u} \mathcal{B}_k^{(1)}(u) du \tag{82}$$

and

$$\mathcal{A}_k^{(0)}(\tau) = \kappa_k \theta_k \int_0^\tau \mathcal{B}_k^{(0)}(u) du; \tag{83}$$

$$\mathcal{A}_k^{(1)}(\tau) = \kappa_k \theta_k \int_0^\tau \mathcal{B}_k^{(1)}(u) du; \tag{84}$$

$$\mathcal{A}_k^{(2)}(\tau) = \kappa_k \theta_k \int_0^\tau \mathcal{B}_k^{(2)}(u) du; \tag{85}$$

$$\mathcal{A}_k^{(3)}(\tau) = \kappa_k \theta_k \int_0^\tau \mathcal{B}_k^{(3)}(u) du. \tag{86}$$

Computing the trivial integrals completes the proof.

8.4 Proof of Proposition (5)

We follow the procedure in [Da Fonseca and Grasselli, 2011]. We suppose an expansion for the integrated implied variance of the form $v = \sigma_{\mathrm{imp}}^2\tau = \zeta_0 + \alpha\zeta_1 +$

$\alpha^2\zeta_2$ and we consider the Black-Scholes formula as a function of the integrated implied variance and the log exchange rate $x = \log S$: $C_{\text{BS}}\left(S(t), K, \sigma, \tau\right) = C_{\text{BS}}\left(x(t), K, \sigma_{imp}^2\tau, \tau\right)$. A Taylor-McLaurin expansion gives us the following:

$$\begin{aligned} C_{\text{BS}}\left(x(t), K, \sigma_{imp}^2\tau, \tau\right) &= C_{\text{BS}}\left(x(t), K, \zeta_0, \tau\right) + \alpha\zeta_1\partial_v C_{\text{BS}}\left(x(t), K, \zeta_0, \tau\right) \\ &\quad + \frac{\alpha^2}{2}\left(2\zeta_2\partial_v C_{\text{BS}}\left(x(t), K, \zeta_0, \tau\right) + \zeta_1^2\partial_{v^2}^2 C_{\text{BS}}\left(x(t), K, \zeta_0, \tau\right)\right). \end{aligned} \tag{87}$$

By comparing this with the price expansion (78) we deduce that the coefficients must be of the form:

$$\zeta_0 = v_0; \tag{88}$$

$$\zeta_1 = \frac{\sum_{k=1}^d \left(\mathcal{A}_k^{(1)}(\tau) + \mathcal{B}_k^{(1)}(\tau)V_k\right)\partial_{xv}^2 C_{\text{BS}}}{\partial_v C_{\text{BS}}}; \tag{89}$$

$$\begin{aligned} \zeta_2 &= \frac{-\zeta_1^2\partial_{vv}^2 C_{\text{BS}} + 2\sum_{k=1}^d \left(\mathcal{A}_k^{(2)}(\tau) + \mathcal{B}_k^{(2)}(\tau)V_k\right)\partial_{vv}^2 C_{\text{BS}}}{2\partial_v C_{\text{BS}}} \\ &+ \frac{2\sum_{k=1}^d \left(\mathcal{A}_k^{(3)}(\tau) + \mathcal{B}_k^{(3)}(\tau)V_k\right)\partial_{xxv}^3 C_{\text{BS}} + \left[\sum_{k=1}^d \left(\mathcal{A}_k^{(1)}(\tau) + \mathcal{B}_k^{(1)}(\tau)V_k\right)\right]^2 \partial_{xxvv}^4 C_{\text{BS}}}{2\partial_v C_{\text{BS}}}, \end{aligned} \tag{90}$$

where the Black-Scholes formula $C_{\text{BS}}\left(x(t), K, \sigma_{imp}^2\tau, \tau\right)$ is evaluated at the point (x, K, v_0, τ). In order to find the values of ζ_1, ζ_2, we differentiate (34)-(37) thus obtaining the following ODE's:

$$\begin{aligned} \frac{\partial\mathcal{B}_k^{(0)}}{\partial\tau} &= -\kappa_k\mathcal{B}_k^{(0)}(\tau) + \left(a_k^i - a_k^j\right)^2; \\ \frac{\partial\mathcal{B}_k^{(1)}}{\partial\tau} &= -\kappa_k\mathcal{B}_k^{(1)}(\tau) + \left(a_k^i - a_k^j\right)\rho_k\xi_k\mathcal{B}_k^{(0)}(\tau); \\ \frac{\partial\mathcal{B}_k^{(2)}}{\partial\tau} &= -\kappa_k\mathcal{B}_k^{(2)}(\tau) + \frac{1}{2}\xi_k^2\mathcal{B}_k^{(0)}(\tau)^2; \\ \frac{\partial\mathcal{B}_k^{(3)}}{\partial\tau} &= -\kappa_k\mathcal{B}_k^{(3)}(\tau) + \left(a_k^i - a_k^j\right)\rho_k\xi_k\mathcal{B}_k^{(1)}(\tau). \end{aligned}$$

We consider a Taylor-McLaurin expansion in terms of τ:

$$\mathcal{B}_k^{(0)}(\tau) = \left(a_k^i - a_k^j\right)^2\tau - \frac{\tau^2}{2}\kappa_k\left(a_k^i - a_k^j\right)^2; \tag{91}$$

$$\mathcal{B}_k^{(1)}(\tau) = \frac{\tau^2}{2}\left(a_k^i - a_k^j\right)^3\rho_k\xi_k - \frac{2}{3}\tau^3\kappa_k\left(a_k^i - a_k^j\right)^3\rho^k\xi^k; \tag{92}$$

$$\mathcal{B}_k^{(2)}(\tau) = \frac{\tau^3}{6}\xi_k^2\left(a_k^i - a_k^j\right)^4; \tag{93}$$

$$\mathcal{B}_k^{(3)}(\tau) = \frac{\tau^3}{6}\left(a_k^i - a_k^j\right)^4\rho_k^2\xi_k^2. \tag{94}$$

Noting from (38)-(41) that $\mathcal{A}_k^{(i)}$ are one order in τ higher than the corresponding $\mathcal{B}_k^{(i)}$, the following approximations hold:

$$\sum_{k=1}^{d}\left(\mathcal{A}_k^{(0)}(\tau)+\mathcal{B}_k^{(0)}(\tau)V_k\right)=\sum_{k=1}^{d}\left(a_k^i-a_k^j\right)V_k\tau+o(\tau); \tag{95}$$

$$\sum_{k=1}^{d}\left(\mathcal{A}_k^{(1)}(\tau)+\mathcal{B}_k^{(1)}(\tau)V_k\right)=\sum_{k=1}^{d}\rho_k\xi_k\left(a_k^i-a_k^j\right)^3V_k\frac{\tau^2}{2}+o(\tau^2); \tag{96}$$

$$\sum_{k=1}^{d}\left(\mathcal{A}_k^{(2)}(\tau)+\mathcal{B}_k^{(2)}(\tau)V_k\right)=\sum_{k=1}^{d}\xi_k^2\left(a_k^i-a_k^j\right)^4V_k\frac{\tau^3}{6}+o(\tau^3); \tag{97}$$

$$\sum_{k=1}^{d}\left(\mathcal{A}_k^{(3)}(\tau)+\mathcal{B}_k^{(3)}(\tau)V_k\right)=\sum_{k=1}^{d}\rho_k^2\xi_k^2\left(a_k^i-a_k^j\right)^4V_k\frac{\tau^3}{6}+o(\tau^3). \tag{98}$$

We introduce two variables: the log- forward moneyness $m_f := \log\left(\frac{Se^{(r^i-r^j)\tau}}{K}\right)$ and $V := \left(\mathbf{a}^i-\mathbf{a}^j\right)^\top \mathrm{Diag}(\mathbf{V})\left(\mathbf{a}^i-\mathbf{a}^j\right)\tau$. Then, from [Lewis, 2000], we consider the following ratios among the derivatives of the Black-Scholes formula:

$$\frac{\partial^2_{xv}C_{\mathrm{BS}}\left(x,K,V,\tau\right)}{\partial_v C_{\mathrm{BS}}\left(x,K,V,\tau\right)}=\frac{1}{2}+\frac{m_f}{V}; \tag{99}$$

$$\frac{\partial^2_{vv}C_{\mathrm{BS}}\left(x,K,V,\tau\right)}{\partial_v C_{\mathrm{BS}}\left(x,K,V,\tau\right)}=\frac{m_f^2}{2V^2}-\frac{1}{2V}-\frac{1}{8}; \tag{100}$$

$$\frac{\partial^3_{xxv}C_{\mathrm{BS}}\left(x,K,V,\tau\right)}{\partial_v C_{\mathrm{BS}}\left(x,K,V,\tau\right)}=\frac{1}{4}+\frac{m_f-1}{V}+\frac{m_f^2}{V^2}; \tag{101}$$

$$\frac{\partial^4_{xxvv}C_{\mathrm{BS}}\left(x,K,V,\tau\right)}{\partial_v C_{\mathrm{BS}}\left(x,K,V,\tau\right)}=\frac{m_f^4}{2V^4}+\frac{m_f^2\left(m_f-1\right)}{2V^3}. \tag{102}$$

Upon substitution of (95)-(102) into (88)-(90), we obtain the values for $\zeta_i, i = 0,1,2$ allowing us to express the expansion of the implied volatility.

$$\zeta_0=\left(\mathbf{a}^i-\mathbf{a}^j\right)^\top\mathrm{Diag}(\mathbf{V})\left(\mathbf{a}^i-\mathbf{a}^j\right)\tau; \tag{103}$$

$$\zeta_1=\left(\sum_{k=1}^{d}\frac{\rho_k\xi_k}{2}\left(a_k^i-a_k^j\right)^4V_k\right)\frac{m_f}{\left(\mathbf{a}^i-\mathbf{a}^j\right)^\top\mathrm{Diag}(\mathbf{V})\left(\mathbf{a}^i-\mathbf{a}^j\right)}\tau; \tag{104}$$

$$\begin{aligned}\zeta_2=&\frac{m_f^2}{\left(\left(\mathbf{a}^i-\mathbf{a}^j\right)^\top\mathrm{Diag}(\mathbf{V})\left(\mathbf{a}^i-\mathbf{a}^j\right)\right)^2}\tau\left[\frac{1}{12}\left(\sum_{k=1}^{d}\xi_k^2\left(a_k^i-a_k^j\right)^4V_k\right)\right.\\&\left.+\frac{1}{6}\left(\sum_{k=1}^{d}\rho_k^2\xi_k^2\left(a_k^i-a_k^j\right)^4V_k\right)-\frac{5}{16}\frac{\left(\sum_{k=1}^{d}\rho_k\xi_k\left(a_k^i-a_k^j\right)^3V_k\right)^2}{\left(\mathbf{a}^i-\mathbf{a}^j\right)^\top\mathrm{Diag}(\mathbf{V})\left(\mathbf{a}^i-\mathbf{a}^j\right)}\right].\end{aligned} \tag{105}$$

9 Images and Tables

	6	5	4	3	2
V_1	0.0137	0.0137	0.0136	0.0137	0.0135
V_2	0.0391	0.0365	0.0278	0.0293	0.0273
a_1^{USD}	0.6650	0.6713	0.6165	0.6371	0.6518
a_2^{USD}	1.0985	1.0531	0.9700	0.9795	0.9514
a_1^{EUR}	1.6177	1.6222	1.5648	1.5804	1.6061
a_2^{EUR}	1.3588	1.3208	1.2746	1.2797	1.2737
a_1^{JPY}	0.2995	0.3151	0.2732	0.3035	0.3116
a_2^{JPY}	1.6214	1.5922	1.5882	1.5858	1.5816
κ_1	0.9418	1.1432	1.5138	1.7349	1.8685
κ_2	1.7909	1.9998	1.9014	0.7142	0.7210
θ_1	0.0370	0.0349	0.0329	0.0329	0.0297
θ_2	0.0909	0.0839	0.0670	0.1236	0.1091
ξ_1	0.4912	0.5138	0.5542	0.5847	0.5962
ξ_2	1.0000	0.9997	0.8736	0.8318	0.8568
ρ_1	0.5231	0.5118	0.4916	0.4727	0.4567
ρ_2	-0.3980	-0.3956	-0.3943	-0.3902	-0.3728
Res. norm.	4.6996e-004	3.4244e-004	1.8618e-004	1.1145e-004	5.2514e-005

Table 1: This table reports the results of the calibration of the model. We concentrate on the two factor case. For each column, a different number of expiries, ranging from 6 to 2, is chosen. More specifically, 6 means that the following expiries are considered: 1, 2, 3, 6, 9 months and 1 year, whereas 5 means that the longest maturity, i.e. 1 year is excluded from the sample. We proceed analogously in the subsequent columns by excluding the longest expiry date up to the point where we perform the calibration on the 2-sample, where we fit the smile at 1 and 2 months. We consider market data as of July 23rd 2010. The reference exchange rates are EURJPY=112.29, EURUSD=1.2921 and USDJPY=86.90. Res. norm. is the residual of the objective function for the given set of parameters.

	5	4	3	2
V_1	0.1244%	-0.2866%	0.0960%	-1.1068%
V_2	-6.5645%	-28.9269%	-25.0960%	-30.0900%
a_1^{USD}	0.9368%	-7.3035%	-4.1928%	-1.9883%
a_2^{USD}	-4.1309%	-11.6957%	-10.8309%	-13.3918%
a_1^{EUR}	0.2745%	-3.2714%	-2.3082%	-0.7190%
a_2^{EUR}	-2.7989%	-6.1962%	-5.8255%	-6.2652%
a_1^{JPY}	5.1809%	-8.8010%	1.3206%	4.0245%
a_2^{JPY}	-1.7985%	-2.0460%	-2.1910%	-2.4522%
κ_1	21.3845%	60.7349%	84.2055%	98.3943%
κ_2	11.6649%	6.1715%	-60.1213%	-59.7402%
θ_1	-5.6226%	-11.1784%	-11.0318%	-19.7810%
θ_2	-7.7145%	-26.3082%	36.0430%	20.0453%
ξ_1	4.6020%	12.8359%	19.0424%	21.3784%
ξ_2	-0.0244%	-12.6344%	-16.8201%	-14.3193%
ρ_1	-2.1702%	-6.0305%	-9.6495%	-12.7003%
ρ_2	-0.6031%	-0.9375%	-1.9522%	-6.3351%

Table 2: In this table we consider the calibration on the largest sample as a basic case. We report the percentage difference between the model parameters resulting from the subsamples

	6	5	4	3	2
V_1	0.0438	0.0430	0.0405	0.0421	0.0412
V_2	0.0465	0.0450	0.0408	0.0370	0.0335
a_1^{USD}	0.7201	0.7165	0.7086	0.7099	0.7082
a_2^{USD}	1.0211	1.0182	1.0095	0.9915	0.9685
a_1^{EUR}	1.2517	1.2534	1.2603	1.2477	1.2538
a_2^{EUR}	1.2624	1.2616	1.2619	1.2575	1.2589
a_1^{JPY}	0.5159	0.5155	0.5093	0.5206	0.5142
a_2^{JPY}	1.5053	1.5083	1.5223	1.5307	1.5372
θ_1	0.1154	0.1169	0.1203	0.1391	0.1300
θ_2	0.1344	0.1377	0.1350	0.1253	0.1081
ξ_1	0.8892	0.8898	0.8992	0.9700	0.9925
ξ_2	0.9338	0.9450	0.9458	0.9616	0.9659
ρ_1	0.5226	0.5132	0.4950	0.4756	0.4591
ρ_2	-0.4042	-0.4030	-0.4004	-0.3887	-0.3721

Table 3: This table reports the results of the calibration of the model. In this case we are assuming $\kappa_k = 1, k = 1, 2$. For each column, a different number of expiries, ranging from 6 to 2, is chosen. Res. norm. is the residual of the objective function for the given set of parameters.

	5	4	3	2
V_1	-1.8915%	-7.6930%	-3.8971%	-5.9284%
V_2	-3.1003%	-12.1687%	-20.3324%	-28.0033%
a_1^{USD}	-0.5056%	-1.6003%	-1.4171%	-1.6497%
a_2^{USD}	-0.2832%	-1.1348%	-2.9033%	-5.1535%
a_1^{EUR}	0.1322%	0.6825%	-0.3164%	0.1703%
a_2^{EUR}	-0.0691%	-0.0438%	-0.3903%	-0.2826%
a_1^{JPY}	-0.0857%	-1.2718%	0.9087%	-0.3396%
a_2^{JPY}	0.1994%	1.1235%	1.6872%	2.1131%
θ_1	1.3740%	4.2649%	20.5911%	12.6966%
θ_2	2.4412%	0.4181%	-6.8073%	-19.5908%
ξ_1	0.0622%	1.1246%	9.0864%	11.6096%
ξ_2	1.1985%	1.2881%	2.9747%	3.4434%
ρ_1	-1.7994%	-5.2886%	-8.9844%	-12.1501%
ρ_2	-0.2922%	-0.9392%	-3.8297%	-7.9304%

Table 4: In this table we consider the calibration on the largest sample as a basic case, when $\kappa_k = 1, k = 1, 2$. We report the percentage difference between the model parameters resulting from the subsamples

	6	5	4	3	2
$k = 1$	-0.1715	-0.1841	-0.2076	-0.2276	-0.2445
$k = 2$	-0.6745	-0.6640	-0.5086	-0.5153	-0.5768

Table 5: For all $k = 1, 2$ and for each sample we report the quantity $2\kappa_k\theta_k - \xi_k^2$. In all cases the quantity is negative and its absolute value is a measure of the violation of the Feller condition.

	USD/EUR	USD/JPY	EUR/JPY
10DC	-0.0006	-0.0002	-0.0027
15DC		0.0003	-0.0017
25DC	-0.0012	0.0005	-0.0005
0	-0.0022	0.0009	0.0021
25DP	-0.0008	0.0012	0.0042
15DP		0.0004	0.0031
10DP	0.0009	-0.0001	0.0011

Table 6: This table reports the raw difference between the market implied volatility and the implied volatility for 1 year, when we calibrate the model to the previous 5 expiries. Blanks on the first column reflect missing market data for 15DC and 15DP.

	USD/EUR	USD/EUR	USD/JPY	USD/JPY	EUR/JPY	EUR/JPY
	9m	1y	9m	1y	9m	1y
10DC	-0.0031	0.0003	-0.0013	-0.0001	-0.0006	-0.0019
15DC			-0.0007	0.0002	0.0008	-0.0012
25DC	-0.0023	-0.0007	0.0004	0.0004	0.0021	-0.0006
0	-0.0021	-0.0021	0.0020	0.0006	0.0036	0.0012
25DP	-0.0010	-0.0007	0.0011	0.0010	0.0028	0.0033
15DP			-0.0008	0.0003	0.0004	0.0025
10DP	-0.0006	0.0015	-0.0014	-0.0000	-0.0026	0.0007

Table 7: This table reports the raw difference between the market implied volatility and the implied volatility for 1 year and 9 months, when we calibrate the model to the previous 4 expiries. Blanks on the first two columns reflect missing market data for 15DC and 15DP.

		USD/EUR	
	6m	9m	1y
10DC	-0.0060	-0.0023	0.0015
25DC	-0.0034	-0.0019	0.0002
0	-0.0018	-0.0020	-0.0017
25DP	-0.0006	-0.0010	-0.0005
10DP	0.0002	-0.0002	0.0019
		USD/JPY	
	6m	9m	1y
10DC	-0.0058	-0.0011	0.0000
15DC	-0.0042	-0.0005	0.0002
25DC	-0.0009	0.0005	-0.0000
0	0.0016	0.0020	0.0000
25DP	0.0004	0.0009	0.0007
15DP	-0.0019	-0.0012	0.0002
10DP	-0.0037	-0.0020	-0.0002
		EUR/JPY	
	6m	9m	1y
10DC	-0.0008	-0.0003	-0.0009
15DC	0.0011	0.0007	-0.0006
25DC	0.0031	0.0015	-0.0005
0	0.0041	0.0025	0.0006
25DP	0.0014	0.0018	0.0026
15DP	-0.0022	-0.0004	0.0019
10DP	-0.0053	-0.0032	0.0003

Table 8: This table reports the raw difference between the market implied volatility and the implied volatility for 1 year, 9 and 6 months, when we calibrate the model to the previous 3 expiries.

USD/EUR

	3m	6m	9m	1y
10DC	-0.0062	-0.0043	-0.0006	0.0031
25DC	-0.0027	-0.0022	-0.0007	0.0010
0	-0.0013	-0.0009	-0.0014	-0.0015
25DP	-0.0006	0.0001	-0.0005	-0.0005
10DP	0.0008	0.0009	0.0003	0.0020

USD/JPY

	3m	6m	9m	1y
10DC	-0.0090	-0.0052	-0.0004	0.0007
15DC	-0.0062	-0.0038	-0.0002	0.0003
25DC	-0.0037	-0.0009	0.0003	-0.0006
0	0.0010	0.0014	0.0015	-0.0011
25DP	-0.0004	0.0006	0.0009	0.0002
15DP	-0.0022	-0.0014	-0.0008	0.0002
10DP	-0.0039	-0.0029	-0.0013	0.0003

EUR/JPY

	3m	6m	9m	1y
10DC	-0.0045	-0.0003	0.0002	-0.0006
15DC	-0.0021	0.0014	0.0009	-0.0007
25DC	0.0010	0.0030	0.0012	-0.0013
0	0.0030	0.0038	0.0019	-0.0008
25DP	0.0009	0.0014	0.0014	0.0016
15DP	-0.0026	-0.0020	-0.0005	0.0013
10DP	-0.0057	-0.0050	-0.0030	-0.0000

Table 9: This table reports the raw difference between the market implied volatility and the implied volatility for 1 year, 9, 6 and 3 months, when we calibrate the model to the previous 2 expiries.

	USD/EUR	USD/JPY	EUR/JPY
10DC	0.0058	0.0030	0.0046
15DC		0.0022	0.0035
25DC	0.0058	0.0009	0.0041
0	0.0035	0.0007	0.0019
25DP	0.0029	0.0024	0.0016
15DP		0.0027	-0.0012
10DP	0.0042	0.0029	-0.0044

Table 10: This table reports the raw difference between the market implied volatility and the implied volatility for 1 year, when we calibrate the model to the previous 5 expiries and $\kappa_k = 1, k = 1, 2$. Blanks on the first column reflect missing market data for 15DC and 15DP.

	USD/EUR	USD/EUR	USD/JPY	USD/JPY	EUR/JPY	EUR/JPY
	9m	1y	9m	1y	9m	1y
10DC	0.0083	0.0092	0.0034	0.0052	0.0073	0.0090
15DC			0.0021	0.0042	0.0061	0.0078
25DC	0.0060	0.0092	0.0005	0.0029	0.0053	0.0079
0	0.0029	0.0066	-0.0000	0.0025	0.0024	0.0050
25DP	0.0033	0.0056	0.0026	0.0044	0.0025	0.0041
15DP			0.0034	0.0049	0.0006	0.0010
10DP	0.0062	0.0067	0.0041	0.0054	-0.0027	-0.0024

Table 11: This table reports the raw difference between the market implied volatility and the implied volatility for 1 year and 9 months, when we calibrate the model to the previous 4 expiries and $\kappa_k = 1, k = 1, 2$. Blanks on the first two columns reflect missing market data for 15DC and 15DP.

		USD/EUR	
	6m	9m	1y
10DC	0.0073	0.0116	0.0131
25DC	0.0042	0.0091	0.0128
0	0.0010	0.0056	0.0100
25DP	0.0020	0.0058	0.0087
10DP	0.0056	0.0088	0.0099
		USD/JPY	
	6m	9m	1y
10DC	0.0025	0.0048	0.0067
15DC	0.0009	0.0030	0.0053
25DC	-0.0013	0.0008	0.0034
0	-0.0028	-0.0004	0.0023
25DP	0.0002	0.0027	0.0048
15DP	0.0013	0.0041	0.0057
10DP	0.0022	0.0053	0.0067
		EUR/JPY	
	6m	9m	1y
10DC	0.0051	0.0114	0.0138
15DC	0.0036	0.0099	0.0123
25DC	0.0022	0.0085	0.0120
0	-0.0001	0.0048	0.0083
25DP	0.0017	0.0047	0.0071
15DP	0.0010	0.0028	0.0040
10DP	-0.0016	-0.0003	0.0006

Table 12: This table reports the raw difference between the market implied volatility and the implied volatility for 1 year, 9 and 6 months, when we calibrate the model to the previous 3 expiries and $\kappa_k = 1, k = 1, 2$.

USD/EUR	3m	6m	9m	1y
10DC	0.0057	0.0085	0.0125	0.0136
25DC	0.0023	0.0042	0.0086	0.0121
0	-0.0018	-0.0000	0.0041	0.0082
25DP	-0.0008	0.0010	0.0043	0.0068
10DP	0.0025	0.0050	0.0077	0.0086

USD/JPY	3m	6m	9m	1y
10DC	0.0013	0.0026	0.0046	0.0063
15DC	0.0004	0.0003	0.0020	0.0040
25DC	-0.0015	-0.0028	-0.0012	0.0010
0	-0.0033	-0.0051	-0.0033	-0.0010
25DP	-0.0010	-0.0015	0.0005	0.0022
15DP	-0.0004	0.0002	0.0025	0.0038
10DP	-0.0002	0.0017	0.0043	0.0053

EUR/JPY	3m	6m	9m	1y
10DC	0.0002	0.0048	0.0106	0.0127
15DC	-0.0009	0.0025	0.0082	0.0101
25DC	-0.0026	-0.0001	0.0056	0.0086
0	-0.0038	-0.0035	0.0008	0.0037
25DP	-0.0008	-0.0007	0.0016	0.0034
15DP	-0.0010	-0.0007	0.0005	0.0012
10DP	-0.0021	-0.0026	-0.0020	-0.0015

Table 13: This table reports the raw difference between the market implied volatility and the implied volatility for 1 year, 9, 6 and 3 months, when we calibrate the model to the previous 3 expiries and $\kappa_k = 1, k = 1, 2$.

Order	$S^{\mathrm{USD,EUR}}$	$S^{\mathrm{JPY,USD}}$	$S^{\mathrm{JPY,EUR}}$
1	$+\infty$	$+\infty$	$+\infty$
2	$+\infty$	12.1962	5.1612
3	$+\infty$	2.9537	2.0580
4	3.3968	1.7990	1.3763
5	2.0070	2.0819	1.0614

Table 14: Times of moment explosions for moments up to order 5 for the three currency pairs.

References

[Andersen and Piterbarg, 2007] Andersen, L. B. G. and Piterbarg, V. V. (2007). Moment explosions in stochastic volatility models. *Finance and Stochastics*, 11:29–50.

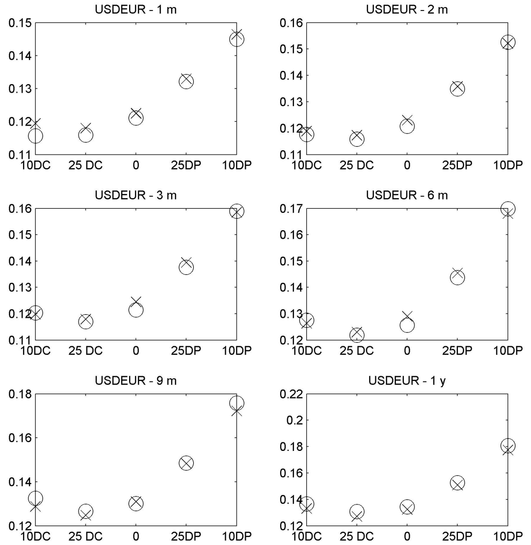

Figure 1: Calibration of USD/EUR implied volatility surface.

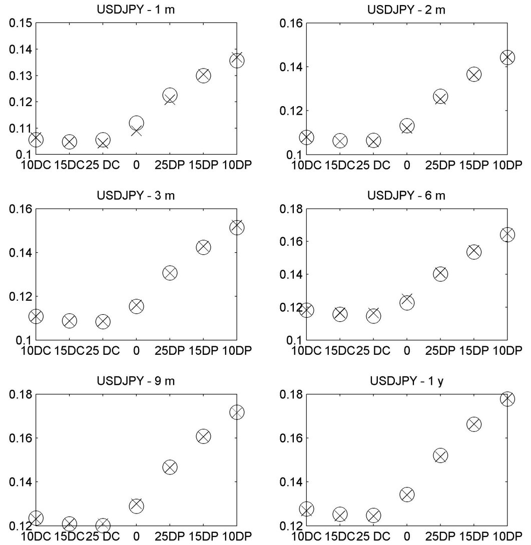

Figure 2: Calibration of USD/JPY implied volatility surface.

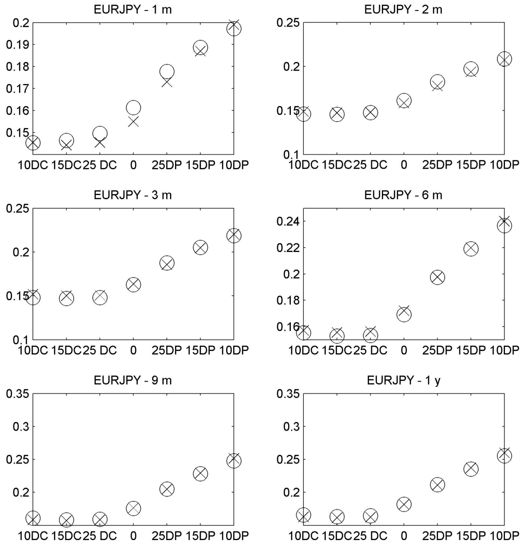

Figure 3: Calibration of EUR/JPY implied volatility surface.

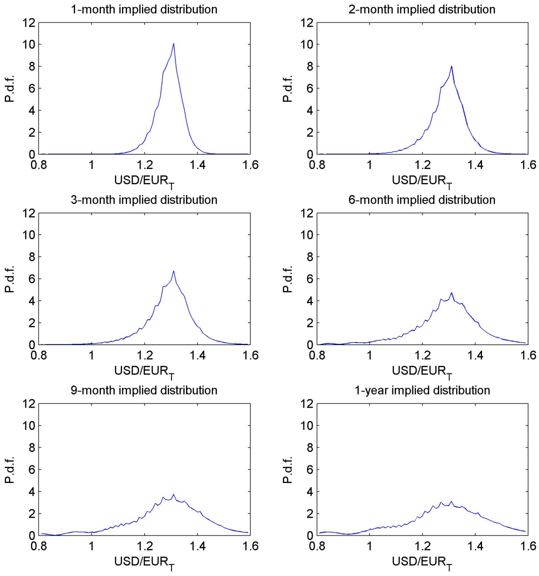

Figure 4: Implied risk-neutral conditional distributions for the USD/EUR exchange rate inferred from option prices.

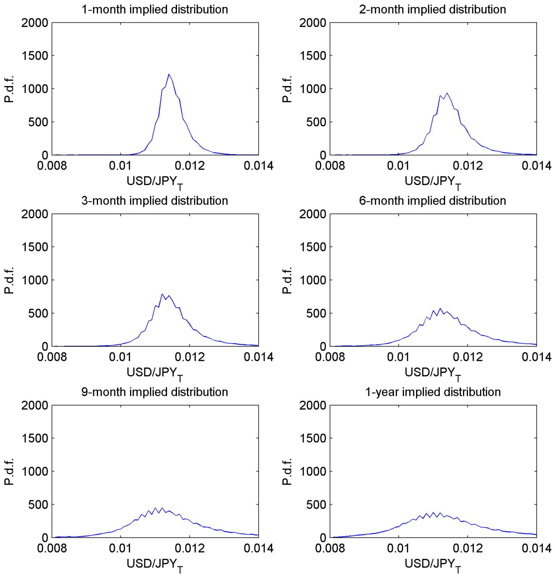

Figure 5: Implied risk-neutral conditional distributions for the USD/JPY exchange rate inferred from option prices.

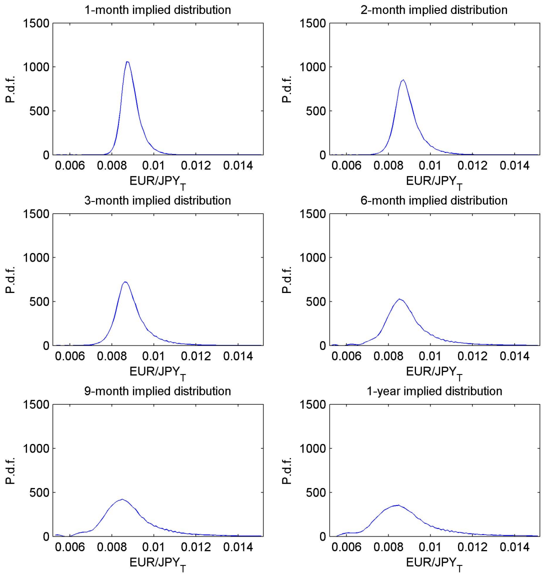

Figure 6: Implied risk-neutral conditional distributions for the EUR/JPY exchange rate inferred from option prices.

[Beneder and Elkenbracht-Huizing, 2003] Beneder, R. and Elkenbracht-Huizing, M. (2003). Foreign exchange options and the volatility smile. *Medium Econometrische Toepassingen*, 2:30–36.

[Björk, 2009] Björk, T. (2009). *Arbitrage theory in continuous time.* Oxford university press, New York, third edition.

[Breeden and Litzenberger, 1978] Breeden, D. and Litzenberger, R. (1978). Prices of State Contingent Claims Implicit in Options Prices. *Journal of Business*, (51(4)):621–651.

[Carr and Madan, 1999] Carr, P. and Madan, D. B. (1999). Option valuation using the fast fourier transform. *Journal of Computational Finance*, 2:61–73.

[Carr and Verma, 2005] Carr, P. and Verma, A. (2005). A joint-heston model for cross-currency option pricing. *Working Paper.*

[Castagna, 2010] Castagna, A. (2010). *FX Options and Smile Risk.* Wiley.

[Christoffersen et al., 2009] Christoffersen, P., Heston, S. L., and Jacobs, K. (2009). The Shape and Term Structure of the Index Option Smirk: Why Multifactor Stochastic Volatility Models Work so Well. *Management Science*, 72:1914–1932.

[Clark, 2011] Clark, I. (2011). *Foreign Exchange Option Pricing: A Practitioner's Guide.* Wiley.

[Cox et al., 1985] Cox, J., Ingersoll, J., and Ross, S. A. (1985). A Theory of the Term Structure of Interest Rates. *Econometrica*, 53:385–407.

[Da Fonseca and Grasselli, 2011] Da Fonseca, J. and Grasselli, M. (2011). Riding on the smiles. *to appear in Quantitative Finance.*

[Del Baño Rollin, 2008] Del Baño Rollin, S. (2008). Spot inversion in the heston model. *Unpublished manuscript, available at http://www.crm.es/Publications/08/Pr837.pdf.*

[Doust, 2007] Doust, P. (2007). The intrinsic currency valuation framework. *Risk*, March:76–81.

[Esquível et al., 2010] Esquível, M. L., Veiga, C., and Wystup, E. (2010). Unifying exotic option closed formulas. *Review of Derivatives Research, forthcoming.*

[Feller, 1951] Feller, W. (1951). Two Singular Diffusion Problems. *Annals of Mathematics*, 54:173–182.

[Garman and Kohlhagen, 1983] Garman, M. B. and Kohlhagen, S. W. (1983). Foreign currency option values. *Journal of International Money and Finance*, 2(3):231 – 237.

[Glasserman and Kim, 2011] Glasserman, K. and Kim, K. (2011). Moment explosions and stationary distributions in affine diffusion models. *forthcoming in Mathematical Finance.*

[Heath and Platen, 2006a] Heath, D. and Platen, E. (2006a). *A Benchmark Approach to Quantitative Finance.* Springer-Verlag.

[Heath and Platen, 2006b] Heath, D. and Platen, E. (2006b). Currency derivatives under a minimal market model. *The ICFAI Journal of Derivatives Marktes*, 3:68–86.

[Heston, 1993] Heston, L. S. (1993). A closed-form solution for options with stochastic volatility with applications to bond and currency options. *Review of Financial Studies*, 6:327–343.

[Karatzas and Shreve, 1991] Karatzas, I. and Shreve, S. E. (1991). *Brownian Motion and Stochastic Calculus.* Springer, Berlin, 2nd edition.

[Keller-Ressel, 2011] Keller-Ressel, M. (2011). Moment explosions and long-term behavior of affine stochastic volatility models. *Mathematical Finance*, 21:73–98.

[Lewis, 2000] Lewis, A. (2000). *Option valuation under stochastic volatility: with Mathematica code.* Finance Press.

[Mijatović and Urusov, 2011] Mijatović, A. and Urusov, M. (2011). On the martingale property of certain local martingales. *to appear in Probability Theory and Related Fields.*

[Qu, 2010] Qu, D. (2010). Pricing Basket Options with Skew. *Willmott Magazine*, pages 58–64.

[Sepp, 2003] Sepp, A. (2003). Fourier Transform for Option Pricing under Affine Jump- Diffusions: An Overview. *Unpublished Manuscript, available at www.hot.ee/seppar.*

[Wong and Heyde, 2004] Wong, B. and Heyde, C. C. (2004). On the martingale property of stochastic exponentials. *Journal of Applied Probability*, 41:654–664.

[Wystup, 2006] Wystup, U. (2006). *FX Options and Structured Products.* Wiley.

[Wystup and Reiswich, 2010] Wystup, U. and Reiswich, D. (2010). A guide to fx options quoting conventions. *The Journal of Derivatives*, 18(2):58–68.